Advances in understanding large-scale responses of the water cycle to climate change

Richard P. Allan (Department of Meteorology and National Centre for Earth Observation, University of Reading, Reading, UK), Mathew Barlow (University of Massachusetts Lowell, USA), Michael P. Byrne (University of St Andrews, UK), Annalisa Cherchi (INGV, Italy), Hervé Douville (CNRM/GMGEC/AMACS, Toulouse, France), Hayley J. Fowler (University of Newcastle, UK), Thian Y. Gan (Univ. Alberta, Canada), Angelina G. Pendergrass (NCAR, USA), Daniel Rosenfeld (The Hebrew University of Jerusalem, Israel), Abigale L. S. Swann (University of Washington, USA), Laura J. Wilcox (University of Reading and National Centre for Atmospheric Science, UK), Olga Zolina (Univ. Grenoble, France)

Abstract

Globally, thermodynamics explains an increases in atmospheric water vapour with warming of around 7% per ºC near to the surface. In contrast, global precipitation and evaporation are constrained by the Earth's energy balance to increase at ~2-3% per ºC. However, this rate of increase is suppressed by rapid atmospheric adjustments in response to greenhouse gases and absorbing aerosols that directly alter the atmospheric energy budget. Rapid adjustments to forcings, cooling effects from scattering aerosol and observational uncertainty can explain why observed global precipitation responses are currently difficult to detect but are expected to emerge and accelerate as warming increases and aerosol forcing diminishes. Precipitation increases with warming are expected to be smaller over land than ocean due to limitations on moisture convergence, exacerbated by feedbacks and affected by rapid adjustments. Thermodynamic increases in atmospheric moisture fluxes amplify wet and dry events, driving an intensification of precipitation extremes. The rate of intensification can deviate from a simple thermodynamic response due to in-storm and larger-scale feedback processes while changes in large-scale dynamics and catchment characteristics further modulate the frequency of flooding in response to precipitation increases. Changes in atmospheric circulation in response to radiative forcing and evolving surface temperature patterns are capable of dominating water cycle changes in some regions. Moreover, the direct impact of human activities on the water cycle through water abstraction, irrigation and land use change are already a significant component of regional water cycle change and are expected to further increase in importance as water demand grows with global population.

Introduction

The global water cycle describes a continual circulation of water through Earth's atmosphere, surface and sub-surface that taps into the vast stores residing in the ocean, large bodies of ice and deep within the ground. This cycle also determines smaller, more transient, yet life-sustaining stores in rivers and lakes, the upper layers of soil and rock as well as within animals and vegetation (Fig. 1a). Precipitation over land is strongly dependent on the transport of water vapour from the ocean (Gimeno et al., 2012) and the return flow is primarily through rivers (Fig. 1b). The water cycle is influenced by natural variations in the sun and volcanic eruptions as well as fluctuations internal to the climate system and there is abundant evidence from the paleoclimate record of substantial past changes (Buckley et al., 2010; Haug et al., 2003; Pederson et al., 2014). Water cycle changes are increasingly becoming dominated by human activities, indirectly through climatic response to emissions of greenhouse gases and aerosol particles but also directly from interference with the land surface and the extraction of water from the ground and river systems (Fig. 1b) for agricultural, industrial and domestic use (Abbott et al., 2019; Asoka et al., 2017; Li et al., 2018).

While global mean precipitation changes are determined by Earth's energy balance, regional changes are dominated by the transport of water vapour and dynamical processes (Gimeno et al., 2012), particularly at scales smaller than ~4000km (Dagan et al., 2019a). Changes in weather patterns are further determined by altering heating and cooling patterns throughout the atmosphere and across the planet's surface. As the climate changes, these competing constraints operating at global and local scales alter key water cycle characteristics, such as precipitation frequency, intensity and duration (Kuo et al., 2015; Pendergrass and Hartmann, 2014b). Future water availability, for use by societies and the ecosystems upon which they depend, is further influenced by increased evaporative demand by the atmosphere (Scheff and Frierson, 2014) but also an increased efficiency of water use by plants in response to elevated CO_2 levels (Lemordant et al., 2018; Milly and Dunne, 2016). Societies experience impacts through localized changes in water availability that are controlled by large-scale atmospheric circulation as well as smaller-scale physical processes. At regional to local scales, water cycle changes therefore result from the interplay between multiple drivers (CO_2, aerosols, land use change and human water use). A primary focus here is on reviewing recent advances in understanding how these complex interactions are expected to determine responses in the global water cycle.

Hydrological sensitivity at the global scale

The Clausius Clapeyron equation is a dominating thermodynamic constraint on atmospheric water vapour. Prevalent increases in atmospheric water vapour with warming (Hartmann et al., 2013) drive powerful amplifying climate feedbacks, intensify atmospheric moisture transport and associated heavy precipitation events and increase atmospheric absorption of sunlight and emission of infrared radiation to the surface that modulate global-scale evaporation and precipitation responses (Boucher et al., 2013; Collins et al., 2013). Simulations and observations confirm a thermodynamic increase in water vapour close to 7 %/ºC at low altitudes when averaged over global scales (Allan et al., 2014). This sensitivity varies depending on the radiative forcing agent and associated warming pattern: for column integrated water vapour it ranges from 6.4±1.5%/ºC[1] for sulphate aerosol forcing to 9.8±3.3%/ºC for black carbon based on idealised modelling (Hodnebrog et al., 2019). Changes over global land are below the thermodynamic response since relative humidity is expected to decrease due to greater land-sea warming contrast (Byrne and O'Gorman, 2018) that is amplified by land surface feedbacks (Berg et al., 2016). Multi-model coupled CMIP5 simulations underestimate declining relative humidity observed over global land (Douville and Plazzotta, 2017; Dunn et al., 2017). This discrepancy also applies to atmosphere-only experiments applying observed sea surface temperature (SST): a single model simulated a -0.05 to -0.25 %/decade trend (1996-2015) compared with an observed estimate of -0.4 to -0.8 %/decade (Dunn et al., 2017). It is not clear if this discrepancy is explained by potential deficiencies in representing ocean to land moisture transport (Vanniere et al., 2018), land-atmosphere coupling (Berg et al., 2016) or inhomogeneity of the observational records (Willett et al., 2014).

[1] 5-95% confidence range is used unless otherwise stated, estimated as 1.645 times standard deviation across models.

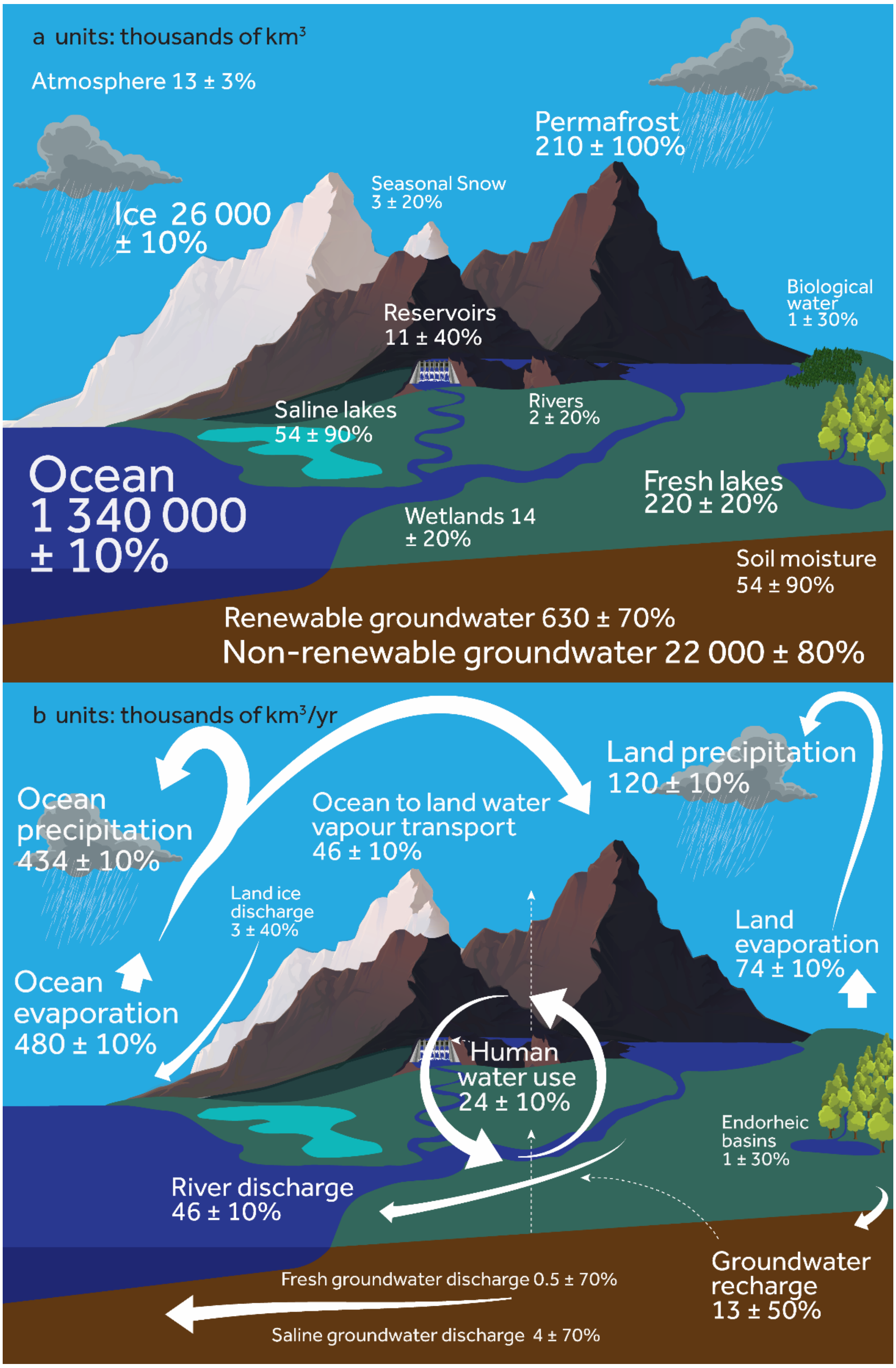

Figure 1: Depiction of the global water cycle: (a) stores (in thousands of km^3) and (b) fluxes (thousands of km^3 per year) based on previous assessments (Abbott et al., 2019; Rodell et al., 2015; Trenberth et al., 2011) with minor adjustments for fresh groundwater flows (Zhou et al., 2019b) and increases in precipitation and evaporation within quoted uncertainty based on observational evidence (Stephens et al., 2012).

In contrast to water vapour, global mean evaporation and precipitation are tightly linked to the atmospheric and surface energy budgets rather than the Clausius Clapeyron equation (O'Gorman et al., 2012; Pendergrass and Hartmann, 2014a). Latent heat released through precipitation is balanced by the net atmospheric longwave radiative cooling minus the heating from absorbed sunlight and sensible heat flux from the surface (Fig. 2a). Complementary energetic arguments apply for surface evaporation (Roderick et al., 2014; Siler et al., 2018). The total global mean precipitation response to warming, or apparent hydrological sensitivity (η_a, Fig.2f) includes fast adjustments that scale with radiative forcing and slow temperature-driven responses to the radiative forcings (Andrews et al., 2010; Bala et al., 2010; Cao et al., 2012). The fast response is caused by near-instantaneous changes in the atmospheric energy budget and atmospheric properties (e.g. temperature, clouds and water vapour; Fig. 2c) in direct response to the radiative effects of a forcing agent (Sherwood et al., 2015). A further relatively fast response involves the land-surface temperature (Fig. 2d) which responds more rapidly to radiative forcing than the ocean (Cao et al., 2012; Dong et al., 2014). The land surface response depends on the partitioning of the increased net surface radiation between latent and sensible heat and, thereby, on the land hydrology and the direct response of plants to elevated CO_2 (Berg et al., 2016; Guerrieri et al., 2019). The slower global temperature-dependent precipitation response, or hydrological sensitivity (η, Fig. 2f), is driven by the increased atmospheric radiative cooling rate of a warming atmosphere (Fig. 2e).

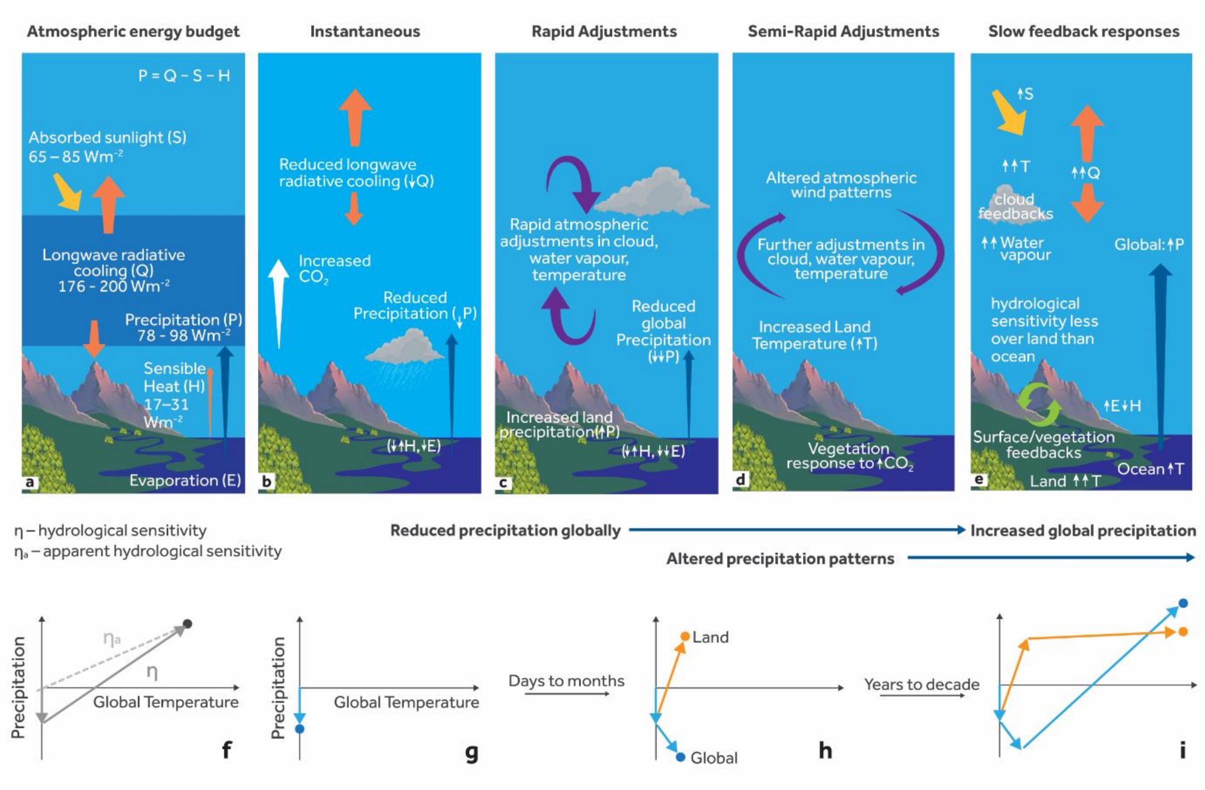

Figure 2: Schematic representation of responses of the atmospheric energy balance and global precipitation to increases in CO2. The energy budget of the atmosphere (a) responds instantaneously to radiative forcings (b) which leads to rapid atmospheric adjustments (c) and slower semi-rapid adjustments involving the land surface and vegetation that further modify atmospheric circulation patterns (d). As the oceans respond to radiative forcing, longer time-scale feedbacks involving the atmosphere, land and oceans alter the surface and atmospheric energy balance, driving increased global evaporation and precipitation (e). This slow response of precipitation to global mean surface temperature is quantified as the hydrological sensitivity, η, while the total precipitation response including initial fast adjustments is termed the apparent hydrological sensitivity, ηa (f). The precipitation response over land and ocean develop over time (g-j) with land hydrological sensitivity tending to be suppressed relative to the global mean.

The fast and slow responses in global precipitation can be illustrated with idealised experiments as part of the 6th phase of the Coupled Model Intercomparison Project (CMIP6) in which atmospheric concentrations of CO_2 are instantaneously quadrupled (Fig. 3; simulations listed in Table 1). Global mean precipitation, relative to a pre-industrial control, increase linearly with global mean temperature (Fig. 3, black dots and line of best fit) at the rate of 2.7%/K and 2.3%/K in the two 4xCO_2 simulations (η, Fig. 2f), consistent with previous estimates of 2.1-3.1 %/K (Fläschner et al., 2016; Samset et al., 2018a). Although relatively well understood physically, idealised modelling has recently uncovered the role of surface evaporation as a limiting factor for the atmospheric warming that determines the magnitude of η (Webb et al., 2018). Climate feedbacks also modulate the magnitude of η (O'Gorman et al., 2012). Model simulations may underestimate η due to deficiencies in the representation of feedbacks from low-altitude cloud (Watanabe et al., 2018) which are linked with hydrological sensitivity through their dependence on temperature lapse rate responses (Webb et al., 2018). Uncertainty in the sensitivity of shortwave absorption by atmospheric water vapour to temperature can explain much of the range in simulated hydrological sensitivity (DeAngelis et al., 2015) although longwave feedbacks also contribute (Richardson et al., 2018a). Consistency in hydrological sensitivity does however disguise contrasting regional responses that are particularly dependent on forcing agent (Richardson et al., 2018a; Samset et al., 2018a).

Data set	Period (this study)	Resolution (lat, lon)	References
HadCRUT4v4.6	1979-2018	5° × 5°	(Morice et al., 2012)
HadCRUH	1979-2003	5° × 5°	(Willett et al., 2008)
SSM/I	1988-2019	0.25° × 0.25°	(Wentz et al., 2007)
ERA5	1979-2019	0.25° × 0.25°	(Copernicus Climate Change Service Climate Data Store (CDS), 2017)
GPCPv2.3	1979-2018	2.5° × 2.5°	(Adler et al., 2017)
AMIP6 simulations	1980-2014		
* Pre-industrial control	30 years		
* 4×CO_2	>150 years		
# Historical	1995–2014		
# SSP2-4.5	2081–2100		
BCC-CSM2-MR		1.125° × 1.125°	(Wu et al., 2019)
BCC-ESM1		2.81° × 2.81°	(Wu et al., 2019)
CanESM5[#]		2.8° × 2.8°	(Swart et al., 2019)
CESM2		0.94° × 1.25°	(Gettelman et al., 2019)
CNRM-CM6-1		1.4° × 1.4°	(Voldoire et al., 2019)
CNRM-ESM2-1		1.4° × 1.4°	(Séférian et al., 2016, 2019)
GFDL-AM4		1.0° × 1.25°	(Zhao et al., 2018b)
GISS-E2-1-G		2.0° × 2.5°	(Elsaesser et al., 2017)
IPSL-CM6A-LR*		1.25° × 2.5°	Servonnat et al., 2020 in prep; Lurton et al., 2020 in prep.
MIROC6		1.406° × 1.406°	(Tatebe et al., 2019)
MRI-ESM2-0*[#]		1.125° × 1.125°	(Yukimoto et al., 2019)
UKESM1-0-LL		1.25° × 1.875°	(Kuhlbrodt et al., 2018)

Table 1: List of observations and simulations with references.

The apparent hydrological sensitivity (η_a) is reduced relative to hydrological sensitivity (η) by greenhouse gases and absorbing aerosols which alter the atmospheric radiation balance, driving rapid adjustments in global precipitation. A rapid adjustment in response to the quadrupling of atmospheric CO_2 concentration is illustrated in Fig. 3: following the black regression line back to the y-axis implies a decrease in global precipitation before global temperatures have begun increasing in response to the elevated CO_2 levels (-4.5%

and -6.8% in the two simulations in Fig. 3). This reflects the rapid adjustments to the atmospheric heating influence of CO_2 radiative forcing, most of which is transferred to the ocean through fast responses in atmospheric vertical motion and circulation. Rapid adjustment effects on precipitation are less certain than the slow responses to surface temperature (Andrews et al., 2010; Bony et al., 2013). The rapid adjustments depend upon how each radiative forcing manifests throughout the atmosphere and surface and explains why the apparent hydrological sensitivity is lower than the hydrological sensitivity for CO_2 forcing (Fig. 2f). Despite uncertainty in the fast precipitation response to radiative forcing, similar spatial patterns are simulated for greenhouse gas, solar and absorbing aerosol radiative forcings (Samset et al., 2016; Xie et al., 2013).

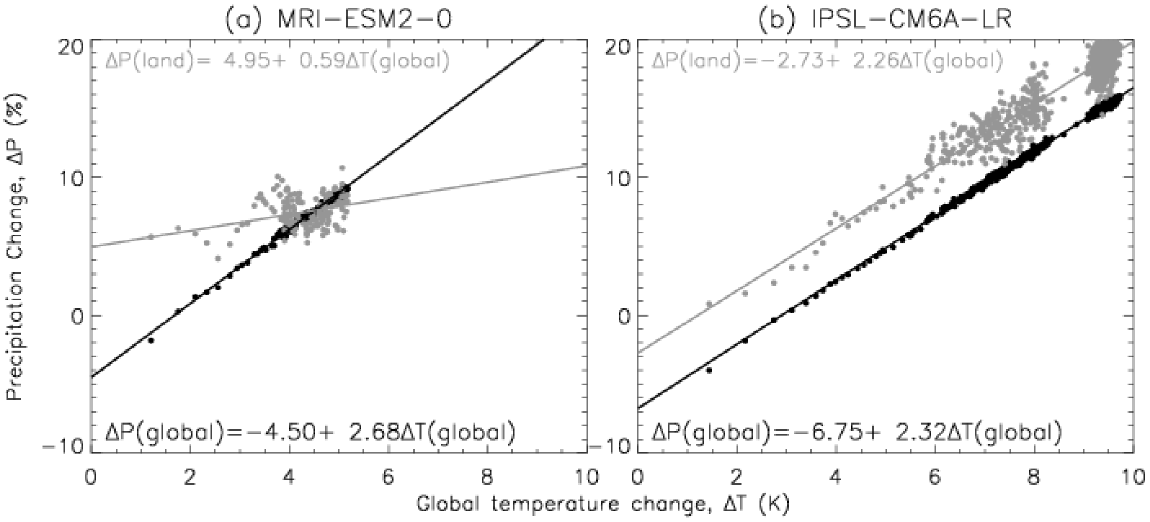

Figure 3: Precipitation changes for global mean (black) and land mean (grey) in response to global mean temperature changes for a $4xCO_2$ experiment relative to a 30-year mean pre-industrial control for (a) MRI-ESM2-0 150 year experiment and (b) IPSL-CM6A-LR 900 year experiment (showing the first 300 and last 300 years) where each dot represents 1 year of data.

Climate drivers that primarily impact the surface rather than atmospheric energy budget initially produce only a small rapid reduction in precipitation. Examples include solar forcing and sulphate aerosol which produce larger η_a than drivers primarily modulating aspects of the atmospheric energy budget such as greenhouse gases and absorbing aerosol (Lin et al., 2018; Liu et al., 2018a; Salzmann, 2016; Samset et al., 2016). Thus, global precipitation appears more sensitive to radiative forcing from sulphate aerosols (2.8±0.7 % per ^oC, $\eta_a \sim \eta$) than greenhouse gases (1.4±0.5 % per ^oC, $\eta_a < \eta$) while the response to black carbon aerosol can be negative (-3.5±5.0 % per ^oC, $\eta_a << \eta$) due to strong atmospheric solar absorption (Samset et al., 2016). In four different climate models, the response to a complete removal of present day anthropogenic aerosol emissions was an increase in global mean precipitation (η_a = 1.6-5.5% per ^oC), mainly attributed to the removal of sulphate aerosol as opposed to other aerosol species (Samset et al., 2018b). η_a also depends on the pattern of aerosol forcing. For example, increased Asian sulphates produce a larger global precipitation response than for comparable aerosol changes over Europe (Liu et al., 2018b). The vertical profile of black carbon and ozone influences the magnitude of the fast global precipitation response yet is more difficult to observe and simulate (Allen and Landuyt, 2014; MacIntosh et al., 2016; Stjern et al., 2017). The range in apparent hydrological sensitivity obtained from 6 simulations of the last glacial maximum and pre-industrial period (η_a=1.6-3.0 %/ ^oC) is greater than for a $4xCO_2$ experiment (η_a=1.3–2.6 %/ ^oC) in which larger CO_2 forcing suppresses precipitation response due to fast adjustments (Li et al., 2013). However, thermodynamic constraints on evaporation and contrasting vegetation and land surface states also play a role. A range of fast precipitation adjustments to CO_2 between models are attributed to the response of vegetation, leading to a repartitioning of surface latent and sensible heat fluxes (DeAngelis et al., 2016).

Hydrological sensitivity is generally suppressed over land (Fig. 2e-i) with a large range (η = 0.8-2.4 %/^oC for

CO_2 doubling experiments) relative to the global mean (η = 2.3-2.7 %/ºC) based on multiple simulations (Richardson et al., 2018a; Samset et al., 2018a). This is partly explained by the greater warming over land than oceans. Since oceans supply much of the moisture to fuel precipitation over land (Findell et al., 2019; Gimeno et al., 2012), the slower ocean warming rate dictates that sufficient moisture cannot be supplied to maintain continental relative humidity (Byrne and O'Gorman, 2018) leading to a drying influence that is further amplified by land surface feedbacks (Berg et al., 2016). A weaker hydrological response over land is important for aridity changes and presents a challenge for attribution of continental precipitation changes to different climate forcings (Samset et al., 2018a).

The distinct response of water cycle responses over land is illustrated in Fig. 3 (grey dots/lines). An implied rapid response in precipitation over land is more positive than the global rapid response in both model simulations. However, one model simulates an initial increase of ~5% over land compared with 4.5% decrease globally (Fig. 3a) while the other model simulates a decrease of ~3% over land compared to a 7% initial decrease globally (Fig. 3b). The more positive initial precipitation response over land than globally can be explained by rapid land warming, in part from increased surface downwelling longwave radiation initially destabilizes the troposphere, strengthening vertical motion, moisture convergence and precipitation over land in the short term (Chadwick et al., 2014; Richardson et al., 2016, 2018a). While the hydrological sensitivity over land is similar to the global response in one model (Fig. 3b: η=2.3%/ºC), the initial rapid increase in precipitation over land in the other simulation (Fig. 3a) is offset over time through a lower hydrological sensitivity over land (η=0.6 %/ºC) compared to the global response (Fig. 3a). Continental precipitation increases as a rapid response to CO_2 have been counteracted by past increases in anthropogenic aerosols which reflect and absorb solar radiation at the expense of surface heating and evaporation of surface moisture (Wild, 2012). The precise response depends upon the aerosol type: sulphate aerosols primarily cool the surface whereas black carbon aerosols absorb sunlight, heating the atmosphere and this effect can dominate over the surface cooling effect (Samset et al., 2016). Recent observations suggest the absorption effects are important in explaining decreases in surface absorbed sunlight that reverse in Europe then China in concert with action to reduce air pollution (Schwarz et al., 2020). Although aerosol cooling effects have opposed rapid precipitation increases in response to direct CO_2 radiative forcing, these counteracting aerosol effects are expected to diminish with future declining aerosol forcing (Acosta Navarro et al., 2017; Richardson et al., 2018a; Rotstayn et al., 2015).

Advances in physical understanding of global precipitation responses can be used to interpret the present day global water cycle changes. Global mean temperature and water vapour are closely coupled (Fig. 4a-b). The linear fit between monthly deseasonalised column integrated water vapour and temperature (1988-2014) is 6.8±0.4 %/ºC in the SSM/I satellite-based observations and 7.1±0.3 %/ºC in an ensemble of 12 atmosphere-only CMIP6 simulations (AMIP6 which apply observed sea surface temperature and sea ice plus realistic radiative forcings; Table 1). This is close to that expected from thermodynamics, assuming small global changes in relative humidity, and is substantially larger than the precipitation sensitivity of 3.2±0.8 %/ºC in GPCP observations and 2.0±0.2 %/ºC in AMIP6 simulations. These are within the range of η from coupled simulations (Fläschner et al., 2016; Samset et al., 2018a) but are not directly comparable since interannual variability depends on cloud feedbacks specific to ENSO-related changes (Stephens et al., 2018). Also shown are the ERA5 reanalysis estimates which, for temperature, show broad consistency with the other datasets. However, the ERA5 depiction of a decrease in water vapour during the early 1990s and larger trends and variability in global precipitation (Fig. 4b-c) are spurious based on analysis of an earlier reanalysis version (Allan et al., 2014) underlining that global-scale water cycle trends in reanalysis products are not realistic.

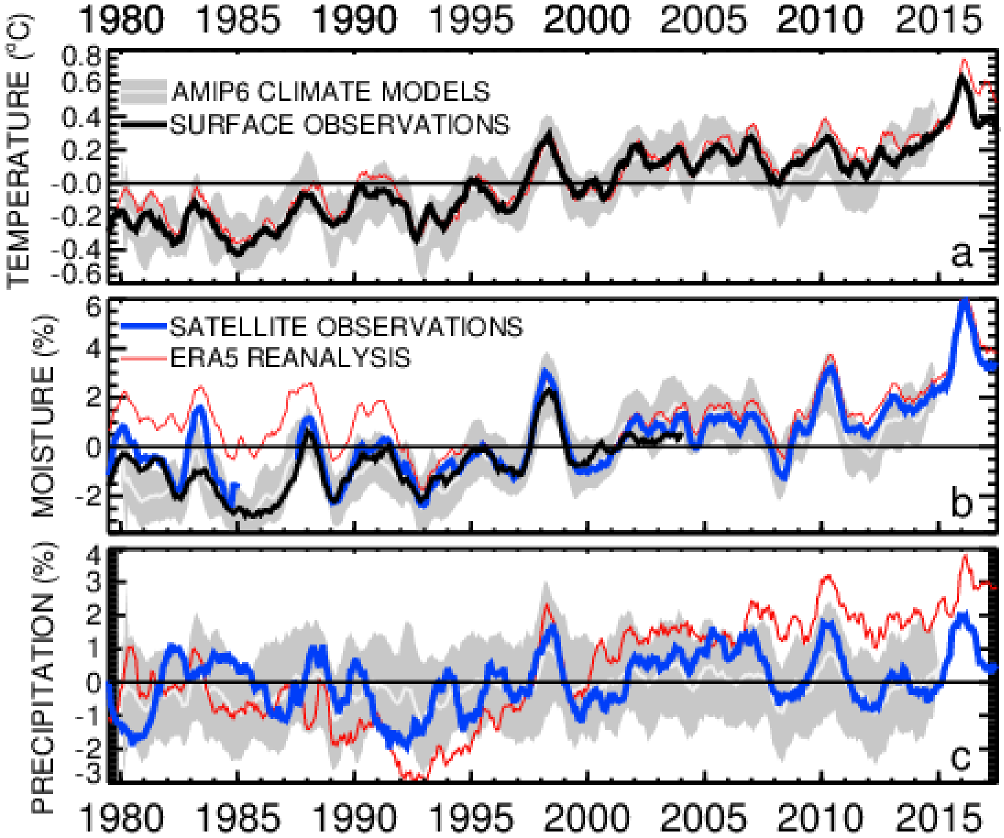

Figure 4: Observed and simulated deseasonalised global mean changes in (a) surface air temperature, (b) column integrated or near surface water vapour and (c) precipitation with 6-month smoothing and 1994-2000 reference period including AMIP6 ensemble mean (white line) with shading representing ±1 standard deviation over 11 models (Table 1) and ERA5 reanalysis (Copernicus Climate Change Service Climate Data Store (CDS), 2017). Observed near surface temperature is from HadCRUTv4.6 (Morice et al., 2012), column integrated water vapour is from SSM/I satellite data (Wentz et al., 2007) over ice free oceans and ERA5 elsewhere, surface near surface specific humidity is from HadCRUH (Willett et al., 2008) and observed precipitation from GPCP v2.3 (Adler et al., 2017) and based on previous methods (Allan et al., 2014).

Longer term trends are more relevant for expected climate change response yet are limited by the observing system. Global mean warming of 0.15±0.01 °C/decade and 1.0±0.1 %/decade increases in moisture in the observations and AMIP6 simulations (1988-2014) imply a water vapour response of 6.7±0.3 %/°C, very close to thermodynamic expectations. Corresponding precipitation trends are not significant at the 95% confidence level in the observations (0.3±0.2 %/decade) and AMIP6 simulations (0.14±0.06 %/decade) though are consistent with the role of fast adjustments suppressing hydrological sensitivity in the near term (Allan et al., 2014; Myhre et al., 2018). The implied apparent hydrological sensitivity (η_a) is 2.0±0.5 %/°C in the observations and 0.9±0.2 %/°C in the simulations. Cooling effects of anthropogenic aerosol and rapid adjustments to increases in greenhouse gases and absorbing aerosol reduce global mean precipitation, offsetting increases relating to the warming climate. Multi-decadal trends in global precipitation for the satellite era are therefore expected to be small and difficult to confirm due to observational uncertainty (Allan et al., 2014) and changes in sensible heat flux become significant in determining the precise global hydrological response (Myhre et al., 2018). The warming influence of continued rises in CO_2 concentration, compounded by declining aerosol cooling, are expected to accelerate increases in global precipitation and its extremes as the slow temperature-related responses dominate over rapid atmospheric adjustments to direct radiative forcing effects as transient climate change progresses (Allan et al., 2014; Lin et al., 2018; Myhre et al., 2018; Salzmann, 2016; Shine et al., 2015; Wilcox et al., 2020). The observational record in Fig. 4 is consistent with physical understanding that global mean precipitation increases more slowly than water vapour content per degree of warming. This has important implications since it determines an increase in water vapour lifetime (Hodnebrog et al., 2019) and altered precipitation characteristics in terms of regional and seasonal duration, frequency and intensity (Pendergrass, 2018).

Thermodynamic constraints on regional precipitation minus evaporation patterns

An important implication of increased atmospheric water vapour with warming (Fig. 4b) is a corresponding intensification of horizontal moisture transport that drives an amplification of existing precipitation minus evaporation (P-E) patterns (Fig. 5). At the regional scale, positive P-E determines fresh water flux from the atmosphere to the surface while negative P-E signifies a net flux of fresh water into the atmosphere. Atmospheric moisture balance achieved primarily by horizontal moisture transport from net evaporative ocean regions into wet convergence zones. At the global scale over the land surface, P-E is positive and balanced by runoff and storage while over the ocean P-E is negative and balanced by runoff from the land (Fig. 1b) with both factors influencing regional salinity.

A projected amplification of P-E zonal mean patterns over the oceans is explained by the thermodynamic scaling of present day simulated P-E (solid and dashed lines in Fig. 5b). This amplification of zonal mean P-E is corroborated by an observed "fresh get fresher, salty get saltier" salinity response to warming (Durack, 2015; Roderick et al., 2014; Skliris et al., 2016). This amplification is moderated by proportionally larger evaporation increases over the sub-tropical oceans relative to the equatorial convergence zones and weakening of the tropical circulation (Chadwick et al., 2013). Suppressed evaporation increases over low latitudes (1% per ^{o}C) are partly explained by rapid adjustments to CO_2 increases and uptake of heat by the ocean compared with high latitudes (Siler et al., 2018). At higher latitudes, evaporation is further increased by the expansion of open water area as sea and lake ice melts with warming (Bintanja and Selten, 2014; Laîné et al., 2014; Sharma et al., 2019; Wang et al., 2018). However, ocean stratification due to heating of the upper layers from radiative forcing is identified as a mechanism for amplifying the salinity patterns beyond the responses driven by water cycle changes alone (Zika et al., 2018). Amplified P-E patterns are additionally reduced by atmospheric and ocean circulation changes that alter the locations of the wettest and therefore freshest ocean regions. Spatial shifts in atmospheric circulation are therefore expected to modify thermodynamic responses locally. This is consistent with paleoclimate evidence showing mean changes are roughly in agreement with thermodynamic scaling (Li et al., 2013) while regional changes are dominated by dynamics (Bhattacharya et al., 2017; D'Agostino et al., 2019; DiNezio and Tierney, 2013; Scheff et al., 2017). However, ice sheet responses also contribute to regional water cycle change over paleoclimate time-scales (Lora, 2018; Morrill et al., 2018; Oster et al., 2015).

Over land, evaporation is regulated by energy fluxes over wet regions, with atmospheric vapour pressure and aerodynamics playing an important role, but for drier regions evaporation is limited by surface water availability (Greve et al., 2014; Roderick et al., 2014). Changes in P-E over drier continental regions are consequently dominated by precipitation changes (Roderick et al., 2014) that are strongly determined by alteration in atmospheric circulation. Projected changes in P-E patterns cannot be simply interpreted as a "wet gets wetter, dry gets drier" response (Byrne and O'Gorman, 2015; Chadwick et al., 2013; Greve et al., 2014; Roderick et al., 2014; Scheff and Frierson, 2015). In a simplistic sense, ocean regions experiencing decreasing P-E cannot meaningfully be described as "dry" (Roderick et al., 2014) and over land "dryness" or aridity is influenced by potential evaporation as well as precipitation (Greve and Seneviratne, 2015; Roderick et al., 2014; Scheff and Frierson, 2015). However, a more fundamental objection to "dry gets drier" over land is that P-E is generally positive and balanced by river discharge over multi-annual time-scales (Fig. 1b) so increased moisture fluxes imply increased P-E with warming (Byrne and O'Gorman, 2015; Greve et al., 2014; Roderick et al., 2014). It is however recognised that P-E may be negative during the tropical dry season or extended dry spells (Kumar et al., 2015) as ground water is lost to a "more thirsty" atmosphere due to greater evaporative demand (Dai et al., 2018; Greve and Seneviratne, 2015; Scheff and Frierson, 2015) and exported remotely. Thus, contrasting water cycle responses are expected for wet and dry periods at the seasonal or sub-seasonal time-scale.

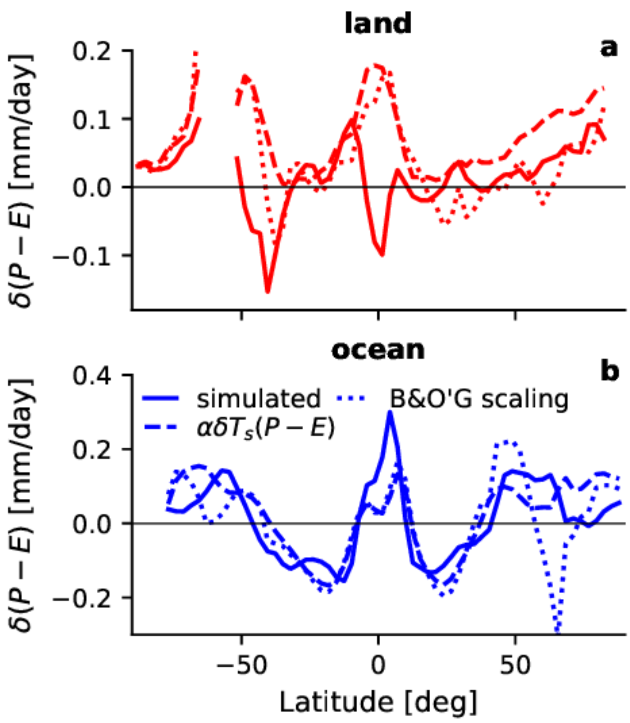

Figure 5: Zonally-averaged changes in precipitation minus evaporation δ(P-E) over (a) land and (b) ocean between the historical (1995–2014) and SSP2-4.5 (2081–2100) simulations (smoothed in latitude using a three-point moving-average filter). The solid lines indicate the simulated changes, which are averages between the CanESM5 and MRI-ESM2-0 models. Dashed lines are a simple thermodynamic scaling, $\alpha\delta T_s$(P-E) and dotted lines show an extended scaling (see Byrne and O'Gorman, 2015).

Decreases in soil moisture over many subtropical land regions are an expected response to a warming climate (Collins et al., 2013). Decreases in P-E over land are explained by reductions in relative humidity driven by increased land-ocean warming contrast and spatial gradients in temperature and humidity (Byrne and O'Gorman, 2015, 2016; Lambert et al., 2017). A simple scaling accounting for these effects captures more closely the simulated responses over subtropical and northern hemisphere land (Fig. 5a). Drying over land is further amplified by vegetation responses (Berg et al., 2016; Byrne and O'Gorman, 2016) and reduces moisture recycling (Findell et al., 2019). The control of soil moisture on evapotranspiration determines feedbacks onto surface climate which vary across simulations (Berg and Sheffield, 2018) and can cause delayed responses over multiple seasons (Kumar et al., 2019).

The response of vegetation to climate change and increased atmospheric CO_2 concentrations also determines regional P-E as well as aridity. Depending on their response, plants may either amplify (Ukkola et al., 2016) or ameliorate (Swann et al., 2016) warming impacts on drought at the surface. Plant water use efficiency is determined by the ratio of photosynthesis to transpiration which in turn is determined by stomatal conductance and vapour pressure deficit. Increased water use efficiency by plants is driven by enhanced photosynthesis and stomatal closure in response to higher CO_2 levels. This can reduce evaporation from vegetated surfaces and exacerbate declining continental relative humidity and precipitation while limiting runoff increases and drying of soils at the root zone (Berg et al., 2017; Berg and Sheffield, 2018; Bonfils et al., 2017; Chadwick et al., 2017; Kooperman et al., 2018a; Lemordant et al., 2018; Mankin et al., 2018; Milly and Dunne, 2016; Peters et al., 2018; Swann et al., 2016). However, increased plant growth in direct response to elevated CO_2 concentrations that also drives greater tolerance to aridity can counteract increased water use efficiency, thereby offsetting the atmospheric drying, runoff increases and soil drying effects (Bonfils et al., 2017; Guerrieri et al., 2019; Lemordant et al., 2018; Mankin et al., 2018, 2019; Milly and Dunne, 2016; Peters et al., 2018; Yang et al., 2018). Plant physiological responses thereby represent an

uncertain component of semi-rapid adjustments to CO_2 forcing (Fig. 2d).
Human activities also directly alter P-E over land. Intensive irrigation increases evapotranspiration and atmospheric water vapour locally. Although increased irrigation efficiency may ensure more water is available to crops, the corresponding reduction in runoff and subsurface recharge may exacerbate hydrologic drought deficits (Grafton et al., 2018). Land use change, including deforestation and urbanisation, can further alter regional P and E through changes in the surface energy and water balance. Direct human interference with the land surface combined with complex surface feedbacks therefore complicate the expected regional water cycle responses over land. Therefore whilst increased moisture transport into wet parts of the atmospheric circulation will amplify P-E patterns globally, the interactions of geography, atmospheric circulation, human activities and feedbacks involving vegetation and soil moisture lead to a complex regional response over land. However, multiple lines of evidence indicate that the contrast between wet and dry meteorological regimes, seasons and events will amplify as moisture fluxes increase in a warming climate (Chadwick et al., 2016; Chavaillaz et al., 2016; Chou et al., 2013; Dong et al., 2018; Ficklin et al., 2019; Kao et al., 2017; Lan et al., 2019; Liu and Allan, 2013; Marvel et al., 2019; Polson and Hegerl, 2017; Zhang and Fueglistaler, 2019)

Large-scale responses in atmospheric circulation patterns

Changes in the large-scale atmospheric circulation dominate regional water cycle changes yet are not as well understood as changes in thermodynamics. Expected large-scale responses in a warming climate are a weakening and broadening of tropical circulation with poleward migration of tropical dry zones and mid-latitude jets (Collins et al., 2013). Land use change and large-scale irrigation also drive local and remote responses in atmospheric circulation and precipitation by altering the surface energy and moisture balance (Alter et al., 2015; De Vrese et al., 2016; Pei et al., 2016; Wang-Erlandsson et al., 2018; Wey et al., 2015). Atmospheric circulation responds rapidly to radiative forcing (Hodnebrog et al., 2016; Li and Ting, 2017; Richardson et al., 2016, 2018b; Samset et al., 2016, 2018a; Tian et al., 2017) and dominates the spatial pattern of precipitation change in response to different drivers (Bony et al., 2013; He and Soden, 2015; Richardson et al., 2016; Tian et al., 2017). Radiative forcings with heterogeneous spatial patterns such as ozone and aerosol (particularly relating to cloud interactions) drive atmospheric circulation changes through spatially and vertically uneven heating and cooling (Dagan et al., 2019b; Patil et al., 2018; Wilcox et al., 2018). These responses are uncertain for aerosol forcing, particularly in the case of black carbon (Sillmann et al., 2019). Robust changes in atmospheric circulation are also driven by slower, evolving patterns of warming including land-ocean contrasts (Bony et al., 2013; He and Soden, 2015; Ma et al., 2018) that are sensitive to model biases (Zhang and Soden, 2019).

A reduced atmospheric overturning circulation is required to reconcile low-level water vapour increases of ~7% per ºC with smaller global precipitation responses of 2-3% per ºC, a consequence of thermodynamic and energy budget constraints (Collins et al., 2013). The slowdown can occur in both the Hadley and Walker circulations, but in most climate models occurs preferentially in the Walker circulation. Paleoclimate simulations and observations support a Walker circulation weakening with warming (DiNezio et al., 2018). However, internal climate variability can temporarily strengthen the Walker circulation over decadal time-scales (L'Heureux et al., 2013; Sohn et al., 2013). Although a weaker Walker circulation is associated with El Niño, the associated regional water cycle impacts are not relevant for climate change responses since the mechanisms driving weakening differ (Pendergrass and Hartmann, 2014b).

There is also a direct link between CO_2 increases and atmospheric circulation response (Plesca et al., 2018; Shaw and Tan, 2018; Xia and Huang, 2017): a rapid 3-4% slowdown of the large-scale tropical circulation in response to instantaneous quadrupling of CO_2 (Plesca et al., 2018) is dominated by reduced tropospheric radiative cooling in sub-tropical ocean subsidence regions (Bony et al., 2013; Merlis, 2015; Richardson et al., 2016). Subsequent surface warming contributes to a slowdown in circulation, the magnitude of which is estimated to reach 12% for a uniform 4ºC SST increase, driven by the enhancement of atmospheric static stability through thermodynamic decreases in temperature lapse rate (Plesca et al., 2018) and an increase in tropopause height (Collins et al., 2013; Wills et al., 2017). The Hadley cell response is mainly manifest as a widening or poleward shift, partly driven by changes in subtropical baroclinicity and an increase in subtropical static stability (e.g., Chemke and Polvani, 2019).

A fundamental component of the Hadley circulation is the Intertropical Convergence Zone **(**ITCZ), the position, width and strength of which determine the location and seasonality of the tropical rain belt. Cross-equatorial energy transport is important in determining the mean ITCZ position and both of these attributes display systematic biases in climate model simulations (Adam et al., 2016; Boos and Korty, 2016; Byrne et al., 2018; Frierson et al., 2013; Loeb et al., 2016; Stephens et al., 2015b) that can also influence tropical precipitation response to warming (Ham et al., 2018; Samanta et al., 2019; Watt-Meyer and Frierson, 2019). Reduced surface sunlight due to aerosol scattering and absorption that preferentially affects the northern hemisphere partially explain a southward shift of the NH tropical edge from the 1950s to the 1980s (Allen et al., 2015; Brönnimann et al., 2015) and the severe drought in the Sahel that peaked in the mid-1980s (Hwang et al., 2013; Undorf et al., 2018). Although changes in hemispheric energy imbalance drive relatively small ($<1^{o}$ latitude, multi-decadal) shifts in the zonally averaged ITCZ position based on observationally constrained simulations (McGee et al., 2014; Wodzicki and Rapp, 2016), short-term (1-2 years) responses to volcanic eruptions and internal variability can produce more rapid changes (Alfaro-Sánchez et al., 2018). Large shifts in the ITCZ ($>1^{o}$ latitude, decades timescale) and regional monsoons are possible following a potential substantial slowdown or collapse of the Atlantic meridional overturning ocean circulation (Kageyama et al., 2013; Parsons et al., 2014).

Although a dynamical understanding of changes in ITCZ width and strength currently lags understanding of the controls on ITCZ position, energetic and dynamic theories have been developed (Byrne and Schneider, 2016b; Dixit et al., 2018; Harrop and Hartmann, 2016; Popp and Silvers, 2017). Weakening circulation with warming (diagnosed as upward mass transport within the global ITCZ divided by its area) results from a complex interplay between strengthened upward motion in the ITCZ core and weakened updrafts at the edges of the ITCZ (Byrne et al., 2018; Lau and Kim, 2015). This leads to a drying tendency on the equatorward edges of the ITCZ (Byrne and Schneider, 2016b) and a moistening tendency in the ITCZ core: stronger ascent in the ITCZ core amplifies the “wet get wetter” response while reduced moisture inflow near the ITCZ edges reduces the “wet gets wetter” response relative to the thermodynamic increase in moisture transport. Overall ITCZ responses have been linked with hemispheric asymmetry in radiative forcing from greenhouse gases and aerosols (Allen et al., 2015; Chung and Soden, 2017; Dong and Sutton, 2015), feedbacks involving clouds (Su et al., 2017, 2019; Talib et al., 2018) and vertical energy stratification (Byrne and Schneider, 2016a; Popp and Silvers, 2017) while changes in the regional tropical rain belt are larger than for the global ITCZ and involve more complex dynamical mechanisms (Denniston et al., 2016; Singarayer et al., 2017) including monsoons.

Monsoon systems represent an integral component of the seasonal shifts the tropical rain belt that affect billions of people through the supply of fresh water for agriculture. Onset, retreat and sub-seasonal characteristics of monsoons are determined by a complex balance between net energy input by radiative and latent heat fluxes and the export of moist static energy. This energy export is determined by contrasting surface heat capacity between ocean and land and modified through changes in atmospheric dynamics, tropical tropospheric stability and land surface properties (Biasutti et al., 2018; Boos and Korty, 2016; D’Agostino et al., 2019). Thermodynamic intensification of moisture transport increase the intensity and area of monsoon rainfall but this is offset by a weakening tropical circulation (Christensen et al., 2013; Endo et al., 2018).

Monsoon systems are sensitive to spatially varying radiative forcing relating to anthropogenic aerosol (Allen et al., 2015; Hwang et al., 2013; Li et al., 2016; Polson et al., 2014) but also greenhouse gases (Dong and Sutton, 2015) and changes in SST patterns (Guo et al., 2016b; Zhou et al., 2019a) that play a strong role by altering cross-equatorial energy transports and land-ocean temperature contrasts. Aerosols affect the monsoon by altering hemispheric temperature gradients and cross-equatorial energy transports but also drive more local changes through altering land-ocean contrasts and changing moisture flux that depend on whether absorbing or scattering aerosol dominate (Persad et al., 2017). Reduced surface sunlight due to aerosol increases over land and the oceanic response to reduced cross-equatorial flow can amplify the northward gradient of SST cooling thereby weakening the Indian monsoon (Krishnan et al., 2016; Patil et al., 2018). Although there has been disagreement between paleoclimate and modern observations, physical theory and numerical simulations of monsoonal changes, many of these discrepancies have been explained by considering regional aspects such as zonal asymmetries in the circulation, land/ocean differences in surface fluxes and the character of convective systems (Bhattacharya et al., 2017, 2018; Biasutti et al., 2018; D'Agostino et al., 2019; Seth et al., 2019).

Poleward expansion of the tropical belt is expected to drive a corresponding shift in mid-latitude storm tracks, yet driving mechanisms differ between hemispheres. Greenhouse gas forcing drives a stronger poleward expansion in the southern hemisphere than the northern hemisphere. In addition, tropospheric ozone and anthropogenic aerosol forcing contribute to the northern hemisphere changes while an amplification of the southern hemisphere response by stratospheric ozone depletion will not apply as ozone levels recover (Allen et al., 2012; Davis et al., 2016; Grise et al., 2019; Watt-Meyer et al., 2019). A thermal gradient between the polar and lower latitude regions that decreases at low levels and increases at upper levels is consistent with a strengthening of the winter jet stream in both hemispheres. However, the precise mechanisms are complex (Vallis et al., 2015) and the influence of amplified Arctic warming on mid-latitude regional water cycles is not well understood based on simple physical grounds due to the large number of competing physical processes (Barnes and Polvani, 2013; Cohen et al., 2014; Henderson et al., 2018; Hoskins and Woollings, 2015; Tang et al., 2014; Woollings et al., 2018). Weakening of the northern hemisphere summer jet stream is thought to potentially amplify wet and dry extremes through increased persistence of weather types (Pfleiderer et al., 2018) and was linked to reduced precipitation in mid-latitudes based on an early Holocene paleoclimate record (Routson et al., 2019). However, recent analysis of observations and coupled climate simulations show little influence of Arctic warming amplification on mid-latitude climate (Blackport and Screen, 2020; Dai and Song, 2020). Regardless of this uncertainty, thermodynamic increases in moisture and convergence within extra-tropical cyclones is a robust driver of precipitation increases within mid-high latitude wet events with implications for more severe flooding.

Changes in characteristics of precipitation and hydrology

Heavy precipitation is expected to become more intense as the planet continues to warm (Fischer and Knutti, 2016; Neelin et al., 2017; O'Gorman, 2015). Increases in low-altitude moisture of around 7% per ^{o}C provide a robust baseline expectation for a similar rate of intensification in extreme precipitation but this is modified by less certain microphysical and dynamical responses (O'Gorman, 2015; Pendergrass et al., 2016; Pfahl et al., 2017) that are space and time-scale dependent (Pendergrass, 2018). The response of streamflow and flooding to changing rainfall characteristics is complex (Fig. 6) and there is not a strong relationship between flood hazard and precipitation at the monthly scale (Emerton et al., 2017; Stephens et al., 2015a). The likelihood of flooding is influenced by snowmelt and antecedent soil moisture (McColl et al., 2017; Wasko and Nathan, 2019; Woldemeskel and Sharma, 2016) that also depend on time and space scales as well as the nature of the land surface. These complex drivers explain regionally dependent increases and decreases in flooding observed over Europe (Berghuijs et al., 2019; Blöschl et al., 2019). Expected drivers of streamflow and flooding are also dependent on direct human intervention such as river catchment management that can include mismanagement leading to infrastructure failure (e.g. reservoirs) as well as detrimental changes in catchment drainage properties or land stability (e.g. mudslides).

Over mid-latitude regions, the amount and intensity of rainfall within extratropical storms is expected to increase with atmospheric moisture. This is particularly evident for atmospheric rivers: long, narrow bands of intense horizontal moisture transport within the warm sector of extratropical cyclones (Dacre et al., 2015; Ralph et al., 2018) that are linked with flooding (Froidevaux and Martius, 2016; Lavers et al., 2011; Paltan et al., 2017; Waliser and Guan, 2017), changes in terrestrial water storage (Adusumilli et al., 2019) and the mass balance of glaciers and snowpack (Little et al., 2019; Mattingly et al., 2018; Oltmanns et al., 2018; Wille et al., 2019). Assuming minor changes in dynamical characteristics, it is expected that increased atmospheric moisture flux will intensify atmospheric river events (Espinoza et al., 2018; Gershunov et al., 2019; Lavers et al., 2013; Ramos et al., 2016). However, changes in location, orientation and dynamical aspects relating to wind speed will dominate responses in some regions.

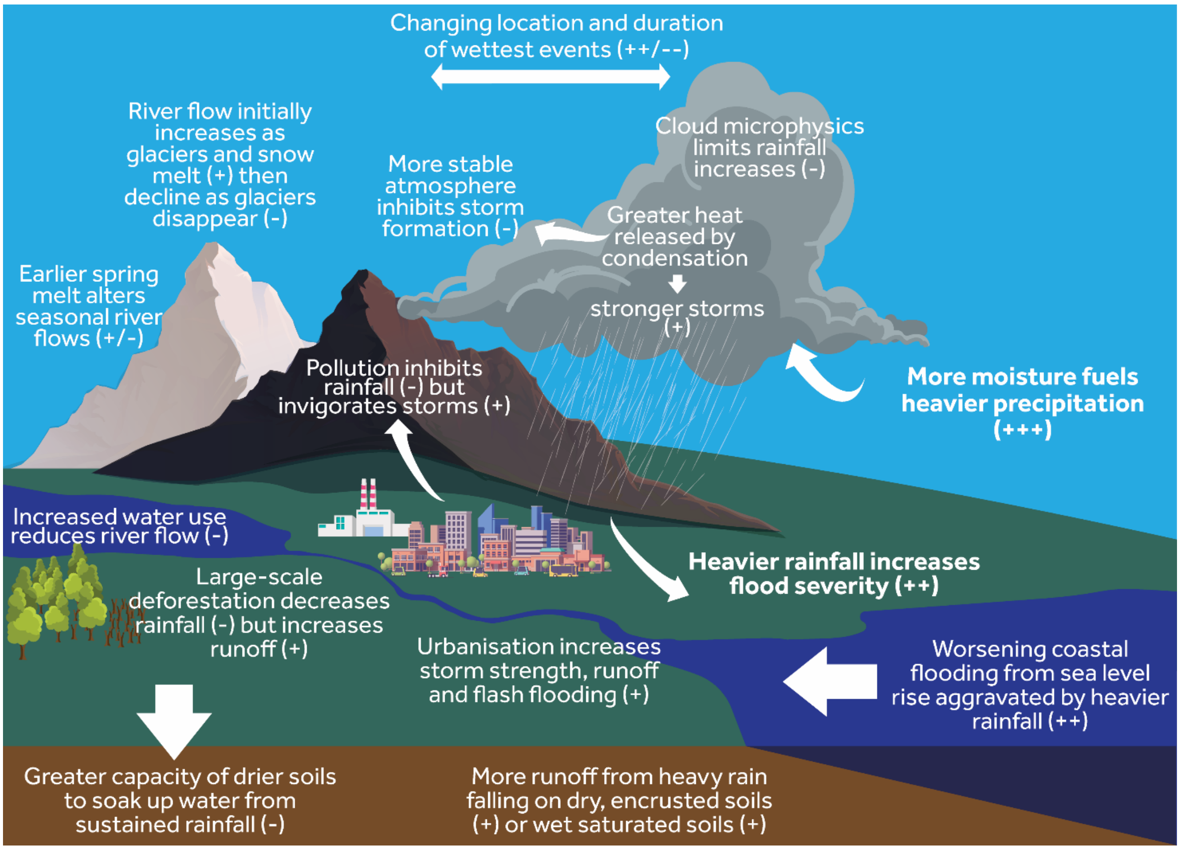

Figure 6: Schematic illustrating factors important in determining changes in heavy precipitation and flooding

Warming is expected to decrease snowfall globally but could drive increases in intensity regionally, particularly in high latitude winter, since heavy snow tends to occur close to the freezing point (O'Gorman, 2014; Turner et al., 2019) which will migrate poleward, in altitude and seasonally. A shorter snow season can be offset by increased snowfall relating to thermodynamic increases in atmospheric moisture (Wu et al., 2018). Warming is expected to reduce rain on snow melt events at lower altitudes due to declining snow cover but increase these events at higher altitudes as snow is replaced by rain (Musselman et al., 2018; Pall et al., 2019). Early but less rapid snowmelt is expected from the reduced available radiative energy earlier in the season (Musselman et al., 2017). Earlier and more extensive winter and spring snowmelt (Zeng et al., 2018) has been further linked with declining summer and autumn runoff in snow-dominated river basins of mid to high latitudes of the Northern Hemisphere (Blöschl et al., 2019; Rhoades et al., 2018). Increased glacier melt and precipitation are expected to contribute to increasing lake levels, as identified for the inner Tibetan Plateau (Lei et al., 2017). In a warming climate, glacier runoff is initially expected to increase due to additional melt before decreasing in the longer term as glacier volume shrinks, with peak runoff already achieved for some smaller glaciers (Hock et al., 2019). Changes in the cryosphere thereby drive regional and seasonal dependent changes in flooding that may alter in magnitude and even sign over longer time-scales.

Increased severity of flooding on larger, more slowly-responding rivers is expected as precipitation increases during persistent wet events over a season. This can occur in mid-latitudes where blocking patterns continually steer extratropical cyclones across large river catchments with groundwater flooding also playing a role (Muchan et al., 2015; Pfleiderer et al., 2018). Catastrophic floods recorded across Europe and Asia have been linked to persistent atmospheric circulation patterns (Lenggenhager et al., 2018; Nikumbh et al., 2019; Takahashi et al., 2015; Zanardo et al., 2019; Zhou et al., 2018). Increased atmospheric moisture will amplify the severity of these events when they occur (Tan et al., 2019) yet changes in occurrence of blocking patterns, stationary waves and jet stream position depend on multiple drivers and so are not well understood (Woollings et al., 2018). Arctic amplification is expected to reduce the low-level latitudinal temperature gradient which implies a slower or less zonal jet stream and potentially longer duration wet or dry events. However, a stronger temperature gradient in the mid-latitude upper troposphere results as the topical upper troposphere warms and the high-latitude lower stratosphere cools. This potentially drives a stronger jet stream and shorter duration but more intense precipitation associated with the passage of extratropical cyclones, as was found to apply for 30-70ºN in CMIP5 projections (Dwyer and O'Gorman, 2017).

A weakening tropical circulation is expected to reduce tropical cyclone system speed thus amplifying thermodynamic intensification of rainfall, though observational evidence for this has been questioned (Kossin, 2018; Lanzante, 2019; Moon et al., 2019b). Associated flooding can exacerbate an increased severity of coastal inundation due to sea level rise (Bevacqua et al., 2019; Zellou and Rahali, 2019). Sensitivity experiments indicate that the most intense rainfall within tropical and extra-tropical cyclones can increase with warming above the Clausius Clapeyron rate (Chauvin et al., 2017; Phibbs and Toumi, 2016). There is also observational evidence (Rosenfeld et al., 2011, 2012; Zhao et al., 2018a) supported by simulations (Khain et al., 2010; Qu et al., 2017; Wang et al., 2014), that ingestion of aerosols into tropical cyclones can invigorate the peripheral rain bands and increase the overall area and precipitation of the storm. This occurs at the expense of air converging into the eyewall, thus may decrease the storm's maximum wind speed by up to one class in the Sapphire Simpson scale. However, large-scale cooling from anthropogenic aerosol has been linked with a decreased frequency of tropical storms over the north Atlantic which reversed at the end of the century as aerosol emissions declined (Dunstone et al., 2013).

Increased seasonality in lower latitudes, with more intense wet seasons (Chou et al., 2013; Dunning et al., 2018; Kumar et al., 2015; Lan et al., 2019; Liu and Allan, 2013), will alter seasonal hydrology. Decreases in precursor soil moisture after more intense dry seasons may increase the timescale over which seasonal rainfall saturates soils and aquifers. Drying of soils can therefore reduce the probability of seasonal flooding, while saturated soils associated with more intense wet seasons can increase waterlogging (Fig. 6). Changes in seasonal flood timing in response to climate variability are found to be more sensitive than for rainfall-based metrics. The median change in flood timing over East Africa between El Niño and La Niña of 53 days (Ficchì and Stephens, 2019) is substantially larger than implied from a rainfall-based estimates of 14 days (Dunning et al., 2016).

Increased land-ocean temperature gradients have been linked with more intense precipitation over the Sahel based on satellite data since the 1980s (Taylor et al., 2017). Surface feedbacks involving soil moisture and vegetation are also expected to modify regional responses over land (Berg et al., 2016), including for active to break phase transition over India (Karmakar et al., 2017; Roxy et al., 2017). The spatial variability in soil moisture has been linked with the timing and location of convective rainfall through altering the partitioning between latent and sensible heating. This has been demonstrated for the Sahel and Europe using satellite data and is not well represented by simulations (Moon et al., 2019a; Taylor, 2015; Taylor et al., 2013). Changes in soil moisture and vegetation can therefore produce varying effects on rainfall location and intensity (Takahashi and Polcher, 2019; Xiang et al., 2018). Antecedent soil moisture conditions are an important modulator of flooding but less so for more severe flood events (Wasko and Nathan, 2019). Defoliation has also been identified as a short-term driver of the regional hydrological cycle with enhanced runoff following a destructive tropical cyclone (Miller et al., 2019). Increased plant water use efficiency in response to elevated CO_2 concentrations is linked with decreased mean precipitation but increased heavy precipitation days over tropical regions (parts of the Andes, western Amazon, central Africa and the Maritime Continent) based on modelling experiments (Skinner et al., 2017). More efficient water use by plants can further cause increasing runoff responses to rainfall, particularly for extremes (Fowler et al., 2019; Kooperman et al., 2018b; Lemordant et al., 2018).

Precipitation and streamflow are also affected directly by human activities and water use can offset and dominate responses to climate change regionally (Tan and Gan, 2015). Deforestation can drive increased streamflow as demonstrated by simulations and observations over the Amazon and East Africa (Dos Santos et al., 2018; Guzha et al., 2018; Levy et al., 2018) although this can be counterbalanced by decreases resulting from irrigation (Hoegh-Guldberg et al., 2019). Large-scale forest clearance can also drive reductions in precipitation, for example for total Amazon deforestation (Lejeune et al., 2015) but with a substantial range (-38 to +5%) across 44 studies (Spracklen and Garcia-Carreras, 2015) with smaller reductions (-2.3 to -1.3%) estimated from observed Amazon deforestation up to 2010. Small-scale deforestation can actually increase precipitation locally (Lawrence and Vandecar, 2015) and alter storm locations. Altered thermodynamic and aerodynamic properties of the land surface from urbanisation can affect precipitation through altered stability and turbulence (Jiang et al., 2016; Pathirana et al., 2014; Sarangi et al., 2018) and are further perturbed through the effect of aerosol pollution on cloud microphysics (Schmid and Niyogi, 2017). Urbanisation also tends to decrease permeability of the surface, leading to increased surface runoff (Chen et al., 2017) and enhanced urban heat island effects are also known to invigorate convection (Dou et al., 2015; Pathirana et al., 2014).

Urban air pollution can invigorate warm base convective storms. The addition of aerosol particles that serve as cloud condensation nuclei (CCN) leads to clouds with more numerous smaller droplets which are slower to coalesce into raindrops. Therefore, clouds in more polluted air masses need to grow deeper to initiate rain (Braga et al., 2017; Freud and Rosenfeld, 2012; Konwar et al., 2012). In clouds with a warm base and depths extending to heights with sub-zero temperatures, rain suppression increases cloud water that can freeze into large ice hydrometeors and produce heavy rain rates. The added latent heat of freezing can further invigorate the clouds (Rosenfeld et al., 2008a; Thornton et al., 2017) but simulations indicate this heating may be compensated by changes in latent heat at different cloud altitudes (Heikenfeld et al., 2019). An additional invigoration mechanism, which works mainly in convective tropical clouds with strong coalescence and warm rain, is caused by small aerosol particles (<0.05 μm) enhancing the condensation efficiency of the vapor (Fan et al., 2018). These cloud invigoration mechanisms redistribute light rainfall from shallow clouds to heavy rainfall from deep clouds. The aerosol convective invigoration effect is non-monotonic, where the invigoration reverses to weakening at aerosol optical depth greater than ~0.3 though the precise value is dependent on the environmental conditions (Koren et al., 2008; Liu et al., 2019; Rosenfeld et al., 2008). This is mainly due reduced surface solar heating due to aerosol effects which propels the convection but also explained by suppression at the cloud edges which begins to dominate at high aerosol loading (Liu et al., 2019). The magnitude of the effect of aerosols acting as ice forming nuclei is poorly known, but likely much smaller than their effects as CCN, except for snow enhancement in shallow orographic clouds (Rauber et al., 2019). Light-absorbing aerosols, like the microphysical effects of CCN, can redistribute rain intensities from light to heavy. Absorbing aerosol radiative effects increase both instability and convective inhibition, which suppresses the small clouds and enhances the large rain cloud systems (Wang et al., 2013). When the instability is released, often triggered by topographical barriers, intense rainfall and flooding can occur (Fan et al., 2015; Guo et al., 2016a). Such trends were found in India (Goswami et al., 2006) and in eastern China during 1970-2010, and shown to be associated with the large increasing amounts of black carbon aerosols there (Guo et al., 2017; Qian et al., 2009).

Recent advances have been made in understanding the expected changes in sub-daily rainfall intensity that can be particularly important in determining flash flooding (Westra et al., 2014). The intensity of convective storms is related to Convective Available Potential Energy (CAPE) which is expected to increase thermodynamically with warming (Barbero et al., 2019; Romps, 2016) although the heaviest rainfall is not necessarily associated with the most intense storms in terms of depth, based on satellite data (Hamada et al., 2015). Intensification can exceed thermodynamic expectations since additional latent heating may invigorate individual storms (Berg et al., 2013; Kendon et al., 2019; Molnar et al., 2015; Nie et al., 2018; Prein et al., 2017; Scoccimarro et al., 2015; Zhang et al., 2018) and an increasing height of the tropopause with warming allows the establishment of larger systems (Lenderink et al., 2017) that can amplify total storm precipitation (Prein et al., 2017). This is corroborated by observed scalings up to 3 times the rate expected from the Clausius Clapeyron equation for multiple regions (Burdanowitz et al., 2019; Formayer and Fritz, 2017; Guerreiro et al., 2018; Lenderink et al., 2017) albeit with low statistical certainty (van der Wiel et al., 2019; Zhou et al., 2016). The relevance of present day relationships to climate change remains questionable (Bao et al., 2017; Zhang et al., 2017) although is improved by considering scaling with dewpoint temperature which reduces dependence on dynamical factors (Ali et al., 2018; Barbero et al., 2017; Lenderink et al., 2017). Increased frequency of rainfall events above a fixed intensity threshold (Myhre et al., 2019) reflect the less severe precipitation events intensifying above the threshold so intensification of heavy rainfall in weather systems remains the dominant mechanism.

Intensification of sub-daily rainfall is inhibited in regions and seasons where available moisture is limited (Prein et al., 2017) and simulations indicate that scaling can depend on time of day (Meredith et al., 2019). However, a fixed threshold temperature above which precipitation is limited by moisture availability is not supported by recent modelling evidence (Neelin et al., 2017; Prein et al., 2017; Zhang and Fueglistaler, 2019). Enhanced latent heating of the atmosphere by more "juicy" storms can also suppress convection at larger-scales due to atmospheric stabilization as demonstrated with high resolution, idealised and large ensemble modelling studies (Chan et al., 2018; Kendon et al., 2019; Loriaux et al., 2017; Nie et al., 2018; Tandon et al., 2018). Large eddy simulations demonstrate that stability controls precipitation intensity, moisture convergence governs storm area fraction while relative humidity determines both intensity and area fraction (Loriaux et al., 2017). Atmospheric stability is also increased by the direct radiative heating effect from higher concentrations of CO_2 (Baker et al., 2018) and aerosol through local effects on the atmospheric energy budget and cloud development. Intensification of short-duration intense rainfall is expected to increase the severity and frequency of flash flooding (Chan et al., 2016; Sandvik et al., 2018) and more intense but less frequent storms (Kendon et al., 2019) are also expected to favour runoff and flash flooding at the expense of recharge since a drier surface reduces percolation from intense rain (Eekhout et al., 2018; Yin et al., 2018).

Recent modelling evidence shows increases in convective precipitation extremes are limited by microphysical processes involving droplet/ice fall speeds (Sandvik et al., 2018; Singh and O'Gorman, 2014). Although instantaneous precipitation extremes are sensitive to microphysical processes, daily extremes are determined more by the degree of convective aggregation in one comparison of idealized model simulations (Bao and Sherwood, 2019). Thus regional processes and their impact on dynamical responses are crucial in determining how regional precipitation intensity and hydrology respond to climate change. Thermodynamic factors are however crucial in determining an intensification of heavy rainfall and associated flooding when extreme events occur.

Conclusions

Based on understanding of thermodynamic processes, corroborated by observations and comprehensive simulations, the global water cycle is expected to intensify with warming in terms of moisture fluxes within the atmosphere and exchanges with the land and ocean surface. This intensification will be offset by a weakening tropical circulation in response to changes in the global energy balance and regional temperature gradients. It is well understood that thermodynamic increases in low-altitude water vapour of about 7%/ºC are larger than the 2-3%/ºC increases in global evaporation and precipitation that are driven by Earth's evolving energy balance in response to warming. The slowing of atmospheric circulation is required to reconcile these contrasting responses that also imply an increased water vapour residence time. Combined with more intense fluxes of moisture, this is expected to manifest as a region and season-dependent shift in the distribution of precipitation characteristics such as intensity, frequency and duration. Increases in aerosols offset some of the warming effects that drive the intensification of the hydrological cycle but this depends on the mix of aerosol species and there are strong regional variations. Regionally, more intense moisture fluxes will drive an amplification of wet and dry seasons and weather events, with the possibility for increased duration or persistence driven by tropical circulation weakening. However, regional increases and decreases in precipitation or aridity are expected to be dominated by spatial shifts in atmospheric wind patterns in many regions that alter the location of the wettest and driest parts of the global circulation yet are less certain than thermodynamic drivers. Local scale effects are further modulated by land surface feedbacks and vegetation responses to rising concentrations of CO_2 as well as direct human interference with the water cycle through water use and land use change.

Recent advances in refining how the water cycle is expected to respond to continued emissions of greenhouse gases and aerosol are as follows:

- Understanding of how global precipitation and evaporation increase as the planet warms has strengthened based on idealised modelling. Precipitation and atmospheric circulation respond rapidly to different radiative forcing agents but with moderate uncertainty. There is greater certainty in the global response to the slower evolving warming patterns.
- It is now recognised that cooling from sulphate aerosol and atmospheric heating due to rising concentrations of absorbing aerosol has countered global precipitation increases due to greenhouse gases and over recent decades. However, the dominating greenhouse gas warming influence is expected to drive substantial future global precipitation increases closer to the hydrological sensitivity of 2-3%/ºC with an additional, temporary acceleration of precipitation increases due to declining aerosol forcing.
- Hydrological sensitivity over land is suppressed relative to the global mean and this has been related to land-ocean warming contrast and surface feedbacks. However, simulated responses are uncertain and do not fully capture the observed magnitude of continental relative humidity decline.
- There is further evidence that amplification of precipitation minus evaporation patterns is robust over the ocean. Understanding of responses over land has been refined beyond an inaccurate wet get wetter, dry get drier response. Now recognised as important are regional thermodynamic responses and feedbacks and how aridity or dryness depends on which aspects of the atmosphere, soil or vegetation are the primary focus.
- There is increasing evidence that the water cycle is intensifying with increased moisture fluxes driving heavier rainfall. Amplified fresh water transport and exchanges between the atmosphere and surface are intensifying wet and dry seasons or weather events.
- Although atmospheric circulation responses are less certain than thermodynamic drivers, evidence for a weaker Walker circulation in a warmer climate has expanded. There is, however, recognition that internal variability can lead to temporary strengthening over a decadal time-scale.
- Thermodynamic amplification of monsoon intensity is offset by a weakening tropical circulation but additional suppression of monsoon precipitation due to reduced solar heating from aerosol is expected to reverse as aerosol emissions decline.
- There have been advances in understanding how hemispheric asymmetries in radiative forcing impact the tropical rain belt with northern hemisphere cooling from sulphate aerosol implicated in a southward shift in the ITCZ associated with the 1980s Sahel drought. Greenhouse gas forcing is now thought to have contributed to the recovery in Sahel rainfall through intensification of the Sahara heat low.
- Recent evidence indicates a limited role for Arctic amplification of warming and the rapid reduction in sea ice area in modifying mid-latitude weather patterns including the frequency of persistent jet stream position that can favour flooding or drought.
- There is a growing appreciation for the role of vegetation and land surface feedbacks on water cycle responses. Understanding of the direct response of plants to elevated CO_2 concentrations has also advanced. Reduced stomatal conductance increases water use efficiency thereby reducing transpiration, atmospheric humidity and local precipitation. This can limit drying of soils and increased streamflow induced by climate change. However, increased photosynthesis and plant growth is also capable of counteracting the effects of increased water use efficiency in some regions for species that are not subject to severe water limitation.
- The role of Atmospheric Rivers in determining regional water stores in the ground and as snow or ice have been highlighted above the known influences on extreme rainfall and flooding.
- There is a greater appreciation of the seasonal complexity in water cycle changes as wet and dry periods intensify but the timing and characteristics of wet seasons, melt events and streamflow evolve over time.
- Non-linear changes in streamflow over multi-decadal time-scales are expected in some regions as accelerated glacier melt is followed by declining glacier volume. This can result in a peak in river discharge that has already been passed in some catchments.
- There have been advances in understanding responses of sub-daily precipitation including the

possibility for storm invigoration through enhanced latent heating within storms but convective inhibition operating at larger scales as heat release stabilises the atmosphere. Responses are thereby dependent on time and space scale though uncertainty remains in modelling storm systems and their aggregation.

- There have been some advances in identifying the role of aerosol in cloud development through initial suppression of precipitation but deepening of clouds that drive convective invigoration in tropical clouds.
- The observed shift of rain intensities from low to high can in some cases also be related to the combined microphysical and radiative effects of aerosol suppressing the small and shallow convective clouds and enhancing the large and deep clouds.
- The role of land-sea temperature gradients, surface feedbacks involving soil moisture and vegetation as well as deforestation in determining the location and intensity convective storms has been highlighted while questions remain as to their representation in models.
- There is not a simple relation between rainfall intensification and flooding though evidence has strengthened that the most severe flooding situations will worsen, especially for smaller catchments and urban environments as well as compounding increased coastal inundation from sea level rise.
- There is now a greater appreciation for the direct impact of human activity on the water cycle through extraction of water from the ground and river systems for irrigation and industrial or domestic use as well as how land use change can alter the surface energy and water balances: for example large-scale deforestation is linked with increased streamflow but also altered wind patterns and reduced precipitation and humidity locally.

Acknowledgements

R.P.A. is funded by the National Centre for Earth Observation and U.K. Natural Environment Research Council SMURPHS Grant (NE/N006054/1). H.J.F. is funded by the Wolfson Foundation and the Royal Society as a Royal Society Wolfson Research Merit Award holder (grant WM140025). A.G.P. was supported by the Regional and Global Model Analysis (RGMA) component of the Earth and Environmental System Modeling Program of the U.S. Department of Energy's Office of Biological & Environmental Research (BER) via National Science Foundation (NSF) IA 1844590 and the National Center for Atmospheric Research, which is a major facility sponsored by the NSF under Cooperative Agreement No. 1947282.

References

Abbott, B. W., Bishop, K., Zarnetske, J. P., Minaudo, C., Chapin, F. S., Krause, S., et al. (2019). Human domination of the global water cycle absent from depictions and perceptions. *Nat. Geosci.* 12. doi:10.1038/s41561-019-0374-y.

Acosta Navarro, J. C., Ekman, A. M. L., Pausata, F. S. R., Lewinschal, A., Varma, V., Seland, Ø., et al. (2017). Future response of temperature and precipitation to reduced aerosol emissions as compared with increased greenhouse gas concentrations. *J. Clim.* 30, 939–954. doi:10.1175/JCLI-D-16-0466.1.

Adam, O., Schneider, T., Brient, F., and Bischoff, T. (2016). Relation of the double-ITCZ bias to the atmospheric energy budget in climate models. *Geophys. Res. Lett.* 43, 7670–7677. doi:10.1002/2016GL069465.

Adler, R. F., Gu, G., Sapiano, M., Wang, J.-J., and Huffman, G. J. (2017). Global Precipitation: Means, Variations and Trends During the Satellite Era (1979-2014). *Surv. Geophys.* 38, 679–699. doi:10.1007/s10712-017-9416-4.

Adusumilli, S., Borsa, A. A., Fish, M. A., McMillan, H. K., and Silverii, F. (2019). A decade of terrestrial water storage changes across the contiguous United States from GPS and GRACE. *Geophys. Res. Lett.* 0. doi:10.1029/2019GL085370.

Alfaro-Sánchez, R., Nguyen, H., Klesse, S., Hudson, A., Belmecheri, S., Köse, N., et al. (2018). Climatic and volcanic forcing of tropical belt northern boundary over the past 800 years. *Nat. Geosci.* 11, 933–

938. doi:10.1038/s41561-018-0242-1.

Ali, H., Fowler, H. J., and Mishra, V. (2018). Global observational evidence of strong linkage between dew point temperature and precipitation extremes. *Geophys. Res. Lett.* doi:10.1029/2018GL080557.

Allan, R. P., Liu, C., Zahn, M., Lavers, D. A., Koukouvagias, E., and Bodas-Salcedo, A. (2014). Physically Consistent Responses of the Global Atmospheric Hydrological Cycle in Models and Observations. *Surv. Geophys.* 35, 533–552. doi:10.1007/s10712-012-9213-z.

Allen, R. J., Evan, A. T., Booth, B. B. B., Allen, R. J., Evan, A. T., and Booth, B. B. B. (2015). Interhemispheric aerosol radiative forcing and tropical precipitation shifts during the late Twentieth Century. *J. Clim.* 28, 8219–8246. doi:10.1175/JCLI-D-15-0148.1.

Allen, R. J., and Landuyt, W. (2014). The vertical distribution of black carbon in CMIP5 models: Comparison to observations and the importance of convective transport. *J. Geophys. Res.* 119, 4808–4835. doi:10.1002/2014JD021595.

Allen, R. J., Sherwood, S. C., Norris, J. R., and Zender, C. S. (2012). Recent Northern Hemisphere tropical expansion primarily driven by black carbon and tropospheric ozone. *Nature* 485, 350–354. doi:10.1038/nature11097.

Alter, R. E., Im, E. S., and Eltahir, E. A. B. (2015). Rainfall consistently enhanced around the Gezira Scheme in East Africa due to irrigation. *Nat. Geosci.* 8, 763–767. doi:10.1038/ngeo2514.

Andrews, T., Forster, P. M., Boucher, O., Bellouin, N., and Jones, A. (2010). Precipitation, radiative forcing and global temperature change. *Geophys. Res. Lett.* 37, n/a--n/a. doi:10.1029/2010GL043991.

Asoka, A., Gleeson, T., Wada, Y., and Mishra, V. (2017). Relative contribution of monsoon precipitation and pumping to changes in groundwater storage in India. *Nat. Geosci.* doi:10.1038/ngeo2869.

Baker, H. S., Millar, R. J., Karoly, D. J., Beyerle, U., Benoit, P., Mitchell, D., et al. (2018). Higher CO 2 concentrations increase extreme event risk in a 1 . 5 ◦ C world. *Nat. Clim. Chang.* 8, 267–283. doi:10.1038/s41558-018-0190-1.

Bala, G., Caldeira, K., and Nemani, R. (2010). Fast versus slow response in climate change: implications for the global hydrological cycle. *Clim. Dyn.* 35, 423–434. doi:10.1007/s00382-009-0583-y.

Bao, J., and Sherwood, S. C. (2019). The Role of Convective Self-Aggregation in Extreme Instantaneous Versus Daily Precipitation. *J. Adv. Model. Earth Syst.* doi:10.1029/2018MS001503.

Bao, J., Sherwood, S. C., Alexander, L. V., and Evans, J. P. (2017). Future increases in extreme precipitation exceed observed scaling rates. *Nat. Clim. Chang.* 7, 128–132. doi:10.1038/nclimate3201.

Barbero, R., Fowler, H. J., Blenkinsop, S., Westra, S., Moron, V., Lewis, E., et al. (2019). A synthesis of hourly and daily precipitation extremes in different climatic regions. *Weather Clim. Extrem.* 26, 100219. doi:10.1016/j.wace.2019.100219.

Barbero, R., Fowler, H. J., Lenderink, G., and Blenkinsop, S. (2017). Is the intensification of precipitation extremes with global warming better detected at hourly than daily resolutions? *Geophys. Res. Lett.* 44, 974–983. doi:10.1002/2016GL071917.

Barnes, E. A., and Polvani, L. (2013). Response of the midlatitude jets, and of their variability, to increased greenhouse gases in the CMIP5 models. *J. Clim.* 26, 7117–7135. doi:10.1175/JCLI-D-12-00536.1.

Berg, A., Findell, K., Lintner, B., Giannini, A., Seneviratne, S. I., Van Den Hurk, B., et al. (2016). Land-atmosphere feedbacks amplify aridity increase over land under global warming. *Nat. Clim. Chang.* 6, 869–874. doi:10.1038/nclimate3029.

Berg, A., and Sheffield, J. (2018). Soil moisture-evapotranspiration coupling in CMIP5 models: Relationship with simulated climate and projections. *J. Clim.* 31, 4865–4878. doi:10.1175/JCLI-D-17-0757.1.

Berg, A., Sheffield, J., and Milly, P. C. D. (2017). Divergent surface and total soil moisture projections under global warming. *Geophys. Res. Lett.* 44, 236–244. doi:10.1002/2016GL071921.

Berg, P., Moseley, C., and Haerter, J. O. (2013). Strong increase in convective precipitation in response to higher temperatures. *Nat. Geosci.* 6, 181–185. doi:10.1038/ngeo1731.

Berghuijs, W. R., Harrigan, S., Molnar, P., Slater, L. J., and Kirchner, J. W. (2019). The Relative Importance of Different Flood-Generating Mechanisms Across Europe. *Water Resour. Res.* 55, 4582–4593. doi:10.1029/2019WR024841.

Bevacqua, E., Maraun, D., Vousdoukas, M. I., Voukouvalas, E., Vrac, M., Mentaschi, L., et al. (2019). Higher probability of compound flooding from precipitation and storm surge in Europe under anthropogenic climate change. *Sci. Adv.* 5, eaaw5531. doi:10.1126/sciadv.aaw5531.

Bhattacharya, T., Tierney, J. E., Addison, J. A., and Murray, J. W. (2018). Ice-sheet modulation of deglacial

North American monsoon intensification. *Nat. Geosci.* doi:10.1038/s41561-018-0220-7.

Bhattacharya, T., Tierney, J. E., and DiNezio, P. (2017). Glacial reduction of the North American Monsoon via surface cooling and atmospheric ventilation. *Geophys. Res. Lett.* doi:10.1002/2017GL073632.

Biasutti, M., Voigt, A., Boos, W. R., Braconnot, P., Hargreaves, J. C., Harrison, S. P., et al. (2018). Global energetics and local physics as drivers of past, present and future monsoons. *Nat. Geosci.* 11, 392–400. doi:10.1038/s41561-018-0137-1.

Bintanja, R., and Selten, F. M. (2014). Future increases in Arctic precipitation linked to local evaporation and sea-ice retreat. *Nature* 509, 479–482. doi:10.1038/nature13259.

Blackport, R., and Screen, J. A. (2020). Insignificant effect of Arctic amplification on the amplitude of midlatitude atmospheric waves. *Sci. Adv.* 6, eaay2880. doi:10.1126/sciadv.aay2880.

Blöschl, G., Hall, J., Viglione, A., Perdigão, R., Parajka, R., Merz, B., et al. (2019). Changing climate both increases and decreases European floods. *Nature* 573, 108–111. doi:10.1038/s41586-019-1495-6.

Bonfils, C., Anderson, G., Santer, B. D., Phillips, T. J., Taylor, K. E., Cuntz, M., et al. (2017). Competing influences of anthropogenic warming, ENSO, and plant physiology on future terrestrial aridity. *J. Clim.* 30, 6883–6904. doi:10.1175/JCLI-D-17-0005.1.

Bony, S., Bellon, G., Klocke, D., Sherwood, S., Fermepin, S., and Denvil, S. (2013). Robust direct effect of carbon dioxide on tropical circulation and regional precipitation. *Nat. Geosci.* 6, 447–451. doi:10.1038/ngeo1799.

Boos, W. R., and Korty, R. L. (2016). Regional energy budget control of the intertropical convergence zone and application to mid-Holocene rainfall. *Nat. Geosci.* 9, 892–897. doi:10.1038/ngeo2833.

Boucher, O., Randall, D., Artaxo, P., Bretherton, C., Feingold, G., Forster, P., et al. (2013). Clouds and Aerosols. *Clim. Chang. 2013 - Phys. Sci. Basis*, 571–658. doi:10.1017/CBO9781107415324.016.

Braga, R. C., Rosenfeld, D., Weigel, R., Jurkat, T., Andreae, M. O., Wendisch, M., et al. (2017). Further evidence for CCN aerosol concentrations determining the height of warm rain and ice initiation in convective clouds over the Amazon basin. *Atmos. Chem. Phys.* 17, 14433–14456.

Brönnimann, S., Fischer, A. M., Rozanov, E., Poli, P., Compo, G. P., Sardeshmukh, P. D., et al. (2015). Southward shift of the northern tropical belt from 1945 to 1980. *Nat. Geosci.* 8, 969–974. doi:10.1038/ngeo2568.

Buckley, B. M., Anchukaitis, K. J., Penny, D., Fletcher, R., Cook, E. R., Sano, M., et al. (2010). Climate as a contributing factor in the demise of Angkor, Cambodia. *Proc. Natl. Acad. Sci.* doi:10.1073/pnas.0910827107.

Burdanowitz, J., Buehler, S. A., Bakan, S., and Klepp, C. (2019). On the sensitivity of oceanic precipitation to sea surface temperature. *Atmos. Chem. Phys. Discuss.*, 1–21. doi:10.5194/acp-2019-136.

Byrne, M. P., and O'Gorman, P. A. (2015). The response of precipitation minus evapotranspiration to climate warming: Why the "Wet-get-wetter, dry-get-drier" scaling does not hold over land. *J. Clim.* 28, 8078–8092. doi:10.1175/JCLI-D-15-0369.1.

Byrne, M. P., and O'Gorman, P. A. (2016). Understanding decreases in land relative humidity with global warming: Conceptual model and GCM simulations. *J. Clim.* 29, 9045–9061. doi:10.1175/JCLI-D-16-0351.1.

Byrne, M. P., and O'Gorman, P. A. (2018). Trends in continental temperature and humidity directly linked to ocean warming. *Proc. Natl. Acad. Sci.* 115, 4863–4868. doi:10.1073/pnas.1722312115.

Byrne, M. P., Pendergrass, A. G., and Rapp, A. D. (2018). Response of the Intertropical Convergence Zone to Climate Change : Location , Width and Strength Precipitation climatology. *Curr. Clim. Chang. Reports*. doi:10.1007/s40641-018-0110-5.

Byrne, M. P., and Schneider, T. (2016a). Energetic constraints on the width of the intertropical convergence zone. *J. Clim.* doi:10.1175/JCLI-D-15-0767.1.

Byrne, M. P., and Schneider, T. (2016b). Narrowing of the ITCZ in a warming climate: Physical mechanisms. *Geophys. Res. Lett.* 43, 11,350-11,357. doi:10.1002/2016GL070396.

Cao, L., Bala, G., and Caldeira, K. (2012). Climate response to changes in atmospheric carbon dioxide and solar irradiance on the time scale of days to weeks. *Environ. Res. Lett.* 7, 34015. doi:10.1088/1748-9326/7/3/034015.

Chadwick, R., Boutle, I., and Martin, G. (2013). Spatial patterns of precipitation change in CMIP5: Why the rich do not get richer in the tropics. *J. Clim.* 26, 3803–3822. doi:10.1175/JCLI-D-12-00543.1.

Chadwick, R., Douville, H., and Skinner, C. B. (2017). Timeslice experiments for understanding regional climate projections: applications to the tropical hydrological cycle and European winter circulation. *Clim. Dyn.* 49, 3011–3029. doi:10.1007/s00382-016-3488-6.

Chadwick, R., Good, P., Andrews, T., and Martin, G. (2014). Surface warming patterns drive tropical rainfall pattern responses to CO_2 forcing on all timescales. *Geophys. Res. Lett.* 41, 610–615. doi:10.1002/2013GL058504.

Chadwick, R., Good, P., Martin, G., and Rowell, D. P. (2016). Large rainfall changes consistently projected over substantial areas of tropical land. *Nat. Clim. Chang.* 6, 177–181. doi:10.1038/nclimate2805.

Chan, S. C., Kendon, E. J., Roberts, N., Blenkinsop, S., and Fowler, H. J. (2018). Large-Scale Predictors for Extreme Hourly Precipitation Events in Convection-Permitting Climate Simulations. *J. Clim.* 31, 2115–2131. doi:10.1175/JCLI-D-17-0404.1.

Chan, S. C., Kendon, E. J., Roberts, N. M., Fowler, H. J., and Blenkinsop, S. (2016). The characteristics of summer sub-hourly rainfall over the southern UK in a high-resolution convective permitting model. *Environ. Res. Lett.* 11, 94024. doi:10.1088/1748-9326/11/9/094024.

Chauvin, F., Douville, H., and Ribes, A. (2017). Atlantic tropical cyclones water budget in observations and CNRM-CM5 model. *Clim. Dyn.* 49, 4009–4021. doi:10.1007/s00382-017-3559-3.

Chavaillaz, Y., Joussaume, S., Bony, S., and Braconnot, P. (2016). Spatial stabilization and intensification of moistening and drying rate patterns under future climate change. *Clim. Dyn.* 47, 951–965. doi:10.1007/s00382-015-2882-9.

Chemke, R., and Polvani, L. M. (2019). Exploiting the abrupt $4 \times CO_2$ scenario to elucidate tropical expansion mechanisms. *J. Clim.* 32, 859–875. doi:10.1175/JCLI-D-18-0330.1.

Chen, J., Theller, L., Gitau, M. W., Engel, B. A., and Harbor, J. M. (2017). Urbanization impacts on surface runoff of the contiguous United States. *J. Environ. Manage.* 187, 470–481. doi:10.1016/j.jenvman.2016.11.017.

Chou, C., Chiang, J. C. H., Lan, C. W. C.-W., Chung, C. H. C.-H., Liao, Y. C. Y.-C., and Lee, C. J. C.-J. C. J. (2013). Increase in the range between wet and dry season precipitation. *Nat. Geosci.* 6, 263–267. doi:10.1038/ngeo1744.

Christensen, J. H., Krishna Kumar, K., Aldrian, E., An, S.-I., Cavalcanti, I. F. A., de Castro, M., et al. (2013). “Climate Phenomena and their Relevance for Future Regional Climate Change,” in *Climate Change 2013: The Physical Science Basis. Contribution of Working Group I to the Fifth Assessment Report of the Intergovernmental Panel on Climate Change*, eds. T. F. Stocker, D. Qin, G.-K. Plattner, M. Tignor, S. K. Allen, J. Boschung, et al. (Cambridge, United Kingdom and New York, NY, USA: Cambridge University Press), 1217–1308. doi:10.1017/CBO9781107415324.028.

Chung, E. S., and Soden, B. J. (2017). Hemispheric climate shifts driven by anthropogenic aerosol-cloud interactions. *Nat. Geosci.* 10, 566–571. doi:10.1038/NGEO2988.

Cohen, J., Screen, J. A., Furtado, J. C., Barlow, M., Whittleston, D., Coumou, D., et al. (2014). Recent Arctic amplification and extreme mid-latitude weather. *Nat. Geosci.* 7, 627–637. doi:10.1038/ngeo2234.

Collins, M., Knutti, R., Arblaster, J., Dufresne, J.-L., Fichefet, T., Friedlingstein, P., et al. (2013). “Long-term Climate Change: Projections, Commitments and Irreversibility,” in *Climate Change 2013: The Physical Science Basis. Contribution of Working Group I to the Fifth Assessment Report of the Intergovernmental Panel on Climate Change*, eds. T. F. Stocker, D. Qin, G.-K. Plattner, M. Tignor, S. K. Allen, J. Boschung, et al. (Cambridge, United Kingdom and New York, NY, USA: Cambridge University Press), 1029–1136. doi:10.1017/CBO9781107415324.024.

Copernicus Climate Change Service Climate Data Store (CDS) (2017). Copernicus Climate Change Service (C3S): ERA5: Fifth generation of ECMWF atmospheric reanalyses of the global climate. *Copernicus Clim. Chang. Serv. ERA5 Fifth Gener. ECMWF Atmos. reanalyses Glob. Clim.* Available at: https://cds.climate.copernicus.eu/cdsapp#!/home [Accessed September 1, 2019].

D’Agostino, R., Bader, J., Bordoni, S., Ferreira, D., and Jungclaus, J. (2019). Northern Hemisphere monsoon response to mid-Holocene orbital forcing and greenhouse gas-induced global warming. *Geophys. Res. Lett.* doi:10.1029/2018GL081589.

Dacre, H. F., Clark, P. A., Martinez-Alvarado, O., Stringer, M. A., and Lavers, D. A. (2015). How Do Atmospheric Rivers Form? *Bull. Am. Meteorol. Soc.* 96, 1243–1255. doi:10.1175/bams-d-14-00031.1.

Dagan, G., Stier, P., and Watson-Parris, D. (2019a). Analysis of the atmospheric water budget for elucidating the spatial scale of precipitation changes under climate change. *Geophys. Res. Lett.* 0, 2019GL084173. doi:10.1029/2019GL084173.

Dagan, G., Stier, P., and Watson-Parris, D. (2019b). Contrasting response of precipitation to aerosol perturbation in the tropics and extra-tropics explained by energy budget considerations. *Geophys. Res. Lett.*, 2019GL083479. doi:10.1029/2019GL083479.

Dai, A., and Song, M. (2020). Little influence of Arctic amplification on mid-latitude climate. *Nat. Clim. Chang.* 10, 231–237. doi:10.1038/s41558-020-0694-3.

Dai, A., Zhao, T., and Chen, J. (2018). Climate Change and Drought: a Precipitation and Evaporation Perspective. *Curr. Clim. Chang. reports* 4, 301–312.

Davis, N. A., Seidel, D. J., Birner, T., Davis, S. M., and Tilmes, S. (2016). Changes in the width of the tropical belt due to simple radiative forcing changes in the GeoMIP simulations. *Atmos. Chem. Phys.* 16, 10083–10095. doi:10.5194/acp-16-10083-2016.

De Vrese, P., Hagemann, S., and Claussen, M. (2016). Asian irrigation, African rain: Remote impacts of irrigation. *Geophys. Res. Lett.* 43, 3737–3745. doi:10.1002/2016GL068146.

DeAngelis, A. M., Qu, X., and Hall, A. (2016). Importance of vegetation processes for model spread in the fast precipitation response to CO_2forcing. *Geophys. Res. Lett.* 43, 12,550-12,559. doi:10.1002/2016GL071392.

DeAngelis, A. M., Qu, X., Zelinka, M. D., and Hall, A. (2015). An observational radiative constraint on hydrologic cycle intensification. *Nature* 528, 249–253. doi:10.1038/nature15770.

Denniston, R. F., Ummenhofer, C. C., Wanamaker, A. D., Lachniet, M. S., Villarini, G., Asmerom, Y., et al. (2016). Expansion and contraction of the Indo-Pacific tropical rain belt over the last three millennia. *Sci. Rep.* 6, 34485. doi:10.1038/srep34485.

DiNezio, P. N., and Tierney, J. E. (2013). The effect of sea level on glacial Indo-Pacific climate. *Nat. Geosci.* 6, 485–491. doi:10.1038/ngeo1823.

DiNezio, P. N., Tierney, J. E., Otto-Bliesner, B. L., Timmermann, A., Bhattacharya, T., Rosenbloom, N., et al. (2018). Glacial changes in tropical climate amplified by the Indian Ocean. *Sci. Adv.* 4, eaat9658.

Dixit, V., Geoffroy, O., and Sherwood, S. C. (2018). Control of ITCZ Width by Low-Level Radiative Heating From Upper-Level Clouds in Aquaplanet Simulations. *Geophys Res Lett* 10, 5788–5797. doi:10.1029/2018GL078292.

Dong, B., and Sutton, R. (2015). Dominant role of greenhouse-gas forcing in the recovery of Sahel rainfall. *Nat. Clim. Chang.* 5, 757–760. doi:10.1038/nclimate2664.

Dong, B., Sutton, R. T., Highwood, E., and Wilcox, L. (2014). The impacts of European and Asian anthropogenic sulfur dioxide emissions on Sahel rainfall. *J. Clim.* 27, 7000–7017. doi:10.1175/JCLI-D-13-00769.1.

Dong, L., Leung, L. R., and Song, F. (2018). Future changes of subseasonal precipitation variability in North America during winter under global warming. *Geophys. Res. Lett.* 45, 12,412-467,476. doi:10.1029/2018GL079900.

Dos Santos, V., Laurent, F., Abe, C., and Messner, F. (2018). Hydrologic response to land use change in a large basin in eastern Amazon. *Water (Switzerland)* 10. doi:10.3390/w10040429.

Dou, J., Wang, Y., Bornstein, R., and Miao, S. (2015). Observed Spatial Characteristics of Beijing Urban Climate Impacts on Summer Thunderstorms. *J. Appl. Meteorol. Climatol.* 54, 94–105. doi:10.1175/JAMC-D-13-0355.1.

Douville, H., and Plazzotta, M. (2017). Midlatitude Summer Drying: An Underestimated Threat in CMIP5 Models? *Geophys. Res. Lett.* 44, 9967–9975. doi:10.1002/2017GL075353.

Dunn, R. J. H., Willett, K. M., Ciavarella, A., and Stott, P. A. (2017). Comparison of land surface humidity between observations and CMIP5 models. *Earth Syst. Dyn.* 8, 719–747. doi:10.5194/esd-8-719-2017.

Dunning, C. M., Black, E., and Allan, R. P. (2018). Later wet seasons with more intense rainfall over Africa under future climate change. *J. Clim.*, JCLI-D-18-0102.1. doi:10.1175/JCLI-D-18-0102.1.

Dunning, C. M., Black, E. C. L., and Allan, R. P. (2016). The onset and cessation of seasonal rainfall over Africa. *J. Geophys. Res.* 121, 11405–11424. doi:10.1002/2016JD025428.

Dunstone, N. J., Smith, D. M., Booth, B. B. B., Hermanson, L., and Eade, R. (2013). Anthropogenic aerosol forcing of Atlantic tropical storms. *Nat. Geosci.* 6, 534–539. doi:10.1038/ngeo1854.

Durack, P. (2015). Ocean Salinity and the Global Water Cycle. *Oceanography* 28, 20–31. doi:10.5670/oceanog.2015.03.

Dwyer, J. G., and O'Gorman, P. A. (2017). Changing duration and spatial extent of midlatitude precipitation extremes across different climates. *Geophys. Res. Lett.* 44, 5863–5871. doi:10.1002/2017GL072855.

Eekhout, J. P. C., Hunink, J. E., Terink, W., and de Vente, J. (2018). Why increased extreme precipitation under climate change negatively affects water security. *Hydrol. Earth Syst. Sci.* 22, 5935–5946. doi:10.5194/hess-22-5935-2018.

Elsaesser, G. S., Del Genio, A. D., Jiang, J. H., and Lier-Walqui, M. van (2017). An improved convective ice parameterization for the NASA GISS global climate model and impacts on cloud ice simulation. *J. Clim.* 30, 317–336. doi:10.1175/JCLI-D-16-0346.1.

Emerton, R., Cloke, H. L., Stephens, E. M., Zsoter, E., Woolnough, S. J., and Pappenberger, F. (2017). Complex picture for likelihood of ENSO-driven flood hazard. *Nat. Commun.* 8, 14796. doi:10.1038/ncomms14796.

Endo, H., Kitoh, A., and Ueda, H. (2018). A Unique Feature of the Asian Summer Monsoon Response to Global Warming: The Role of Different Land–Sea Thermal Contrast Change between the Lower and Upper Troposphere. *SOLA* 14, 57–63. doi:10.2151/sola.2018-010.

Espinoza, V., Waliser, D. E., Guan, B., Lavers, D. A., and Ralph, F. M. (2018). Global Analysis of Climate Change Projection Effects on Atmospheric Rivers. *Geophys. Res. Lett.* 45, 4299–4308. doi:10.1029/2017GL076968.

Fan, J., Rosenfeld, D., Yang, Y., Zhao, C., Ruby Leung, L., and Li, Z. (2015). Substantial contribution of anthropogenic air pollution to catastrophic floods in Southwest China. *Geophys. Res. Lett.* 42, 6066–6075. doi:10.1002/2015GL064479.

Ficchì, A., and Stephens, L. (2019). Climate variability alters flood timing across Africa. *Geophys. Res. Lett.*, 2019GL081988. doi:10.1029/2019GL081988.

Ficklin, D. L., Abatzoglou, J. T., and Novick, K. A. (2019). A New Perspective on Terrestrial Hydrologic Intensity That Incorporates Atmospheric Water Demand. *Geophys. Res. Lett.* 46, 8114–8124. doi:10.1029/2019gl084015.

Findell, K. L., Keys, P. W., van der Ent, R. J., Lintner, B. R., Berg, A., and Krasting, J. P. (2019). Rising Temperatures Increase Importance of Oceanic Evaporation as a Source for Continental Precipitation. *J. Clim.* 32, 7713–7726. doi:10.1175/jcli-d-19-0145.1.

Fischer, E. M., and Knutti, R. (2016). Observed heavy precipitation increase confirms theory and early models. *Nat. Clim. Chang.* 6, 986–991. doi:10.1038/nclimate3110.

Fläschner, D., Mauritsen, T., and Stevens, B. (2016). Understanding the intermodel spread in global-mean hydrological sensitivity. *J. Clim.* 29, 801–817. doi:10.1175/JCLI-D-15-0351.1.

Formayer, H., and Fritz, A. (2017). Temperature dependency of hourly precipitation intensities – surface versus cloud layer temperature. *Int. J. Climatol.* 37, 1–10. doi:10.1002/joc.4678.

Fowler, M. D., Kooperman, G. J., Randerson, J. T., and Pritchard, M. S. (2019). Identifying the effect of plant-physiological responses to rising CO_2 on global streamflow. *Nat. Clim. Chang.* 9, 873–879. doi:10.1038/s41558-019-0602-x.

Freud, E., and Rosenfeld, D. (2012). Linear relation between convective cloud drop number concentration and depth for rain initiation. *J. Geophys. Res. Atmos.* 117.

Frierson, D. M. W., Hwang, Y. T., Fučkar, N. S., Seager, R., Kang, S. M., Donohoe, A., et al. (2013). Contribution of ocean overturning circulation to tropical rainfall peak in the Northern Hemisphere. *Nat. Geosci.* 6, 940–944. doi:10.1038/ngeo1987.

Froidevaux, P., and Martius, O. (2016). Exceptional integrated vapour transport toward orography: an important precursor to severe floods in Switzerland. *Q. J. R. Meteorol. Soc.* 142, 1997–2012. doi:10.1002/qj.2793.

Gershunov, A., Shulgina, T. M., Clemesha, R. E. S., Guirguis, K., Pierce, D. W., Dettinger, M. D., et al. (2019). “Precipitation regime change in Western North America: The role of Atmospheric Rivers,” in *Nature Communications* (submitted).

Gettelman, A., Hannay, C., Bacmeister, J. T., Neale, R. B., Pendergrass, A. G., Danabasoglu, G., et al. (2019). High Climate Sensitivity in the Community Earth System Model Version 2 (CESM2). *Geophys. Res. Lett.* 46, 8329–8337. doi:10.1029/2019gl083978.

Gimeno, L., Stohl, A., Trigo, R. M., Dominguez, F., Yoshimura, K., Yu, L., et al. (2012). Oceanic and terrestrial sources of continental precipitation. *Rev. Geophys.* 50, 1–41. doi:10.1029/2012RG000389.1.INTRODUCTION.

Goswami, B. N., Venugopal, V., Sangupta, D., Madhusoodanan, M. S., and Xavier, P. K. (2006). Increasing trend of extreme rain events over India in a warming environment. *Science (80-.).* 314, 1442–1445.

doi:10.1126/science.1132027.

Grafton, R. Q., Williams, J., Perry, C. J., Molle, F., Ringler, C., Steduto, P., et al. (2018). The paradox of irrigation efficiency. *Science (80-.).* 361, 748–750.

Greve, P., Orlowsky, B., Mueller, B., Sheffield, J., Reichstein, M., and Seneviratne, S. I. (2014). Global assessment of trends in wetting and drying over land. *Nat. Geosci.* 7, 716–721. doi:10.1038/NGEO2247.

Greve, P., and Seneviratne, S. I. (2015). Assessment of future changes in water availability and aridity. *Geophys. Res. Lett.* 42, 5493–5499. doi:10.1002/2015GL064127.Received.

Grise, K. M., Davis, S. M., Simpson, I. R., Waugh, D. W., Fu, Q., Allen, R. J., et al. (2019). Recent Tropical Expansion: Natural Variability or Forced Response? *J. Clim.* 32, 1551–1571. doi:10.1175/JCLI-D-18-0444.1.

Guerreiro, S. B., Fowler, H. J., Barbero, R., Westra, S., Lenderink, G., Blenkinsop, S., et al. (2018). Detection of continental-scale intensification of hourly rainfall extremes. *Nat. Clim. Chang.* 8, 803–807. doi:10.1038/s41558-018-0245-3.

Guerrieri, R., Belmecheri, S., Ollinger, S. V., Asbjornsen, H., Jennings, K., Xiao, J., et al. (2019). Disentangling the role of photosynthesis and stomatal conductance on rising forest water-use efficiency. *Proc. Natl. Acad. Sci. U. S. A.* 116, 16909–16914. doi:10.1073/pnas.1905912116.

Guo, J., Deng, M., Lee, S. S., Wang, F., Li, Z., Zhai, P., et al. (2016a). Delaying precipitation and lightning by air pollution over the Pearl River Delta. Part I: Observational analyses. *J. Geophys. Res. Atmos.* 121, 6472–6488. doi:10.1002/2015JD023257.

Guo, J., Su, T., Li, Z., Miao, Y., Li, J., Liu, H., et al. (2017). Declining frequency of summertime local-scale precipitation over eastern China from 1970 to 2010 and its potential link to aerosols. *Geophys. Res. Lett.* 44, 5700–5708. doi:10.1002/2017GL073533.

Guo, L., Turner, A. G., and Highwood, E. J. (2016b). Local and remote impacts of aerosol species on indian summer monsoon rainfall in a GCM. *J. Clim.* 29, 6937–6955. doi:10.1175/JCLI-D-15-0728.1.

Guzha, A. C., Rufino, M. C., Okoth, S., Jacobs, S., and Nóbrega, R. L. B. (2018). Impacts of land use and land cover change on surface runoff, discharge and low flows: Evidence from East Africa. *J. Hydrol. Reg. Stud.* 15, 49–67. doi:10.1016/j.ejrh.2017.11.005.

Ham, Y. G., Kug, J. S., Choi, J. Y., Jin, F. F., and Watanabe, M. (2018). Inverse relationship between present-day tropical precipitation and its sensitivity to greenhouse warming. *Nat. Clim. Chang.* 8, 64–69. doi:10.1038/s41558-017-0033-5.

Hamada, A., Takayabu, Y. N., Liu, C., and Zipser, E. J. (2015). Weak linkage between the heaviest rainfall and tallest storms. *Nat. Commun.* 6, 6213. doi:10.1038/ncomms7213.

Harrop, B. E., and Hartmann, D. L. (2016). The role of cloud radiative heating in determining the location of the ITCZ in aquaplanet simulations. *J. Clim.* doi:10.1175/JCLI-D-15-0521.1.

Hartmann, D. L., Klein Tank, A. M. G., Rusticucci, M., Alexander, L. V, Brönnimann, S., Charabi, Y., et al. (2013). "Observations: Atmosphere and Surface," in *Climate Change 2013: The Physical Science Basis. Contribution of Working Group I to the Fifth Assessment Report of the Intergovernmental Panel on Climate Change*, eds. T. F. Stocker, D. Qin, G.-K. Plattner, M. Tignor, S. K. Allen, J. Boschung, et al. (Cambridge, United Kingdom and New York, NY, USA: Cambridge University Press), 159–254. doi:10.1017/CBO9781107415324.008.

Haug, G. H., Günther, D., Peterson, L. C., Sigman, D. M., Hughen, K. A., and Aeschlimann, B. (2003). Climate and the collapse of Maya civilization. *Science (80-.).* doi:10.1126/science.1080444.

He, J., and Soden, B. J. (2015). Anthropogenic weakening of the tropical circulation: The relative roles of direct CO2 forcing and sea surface temperature change. *J. Clim.* 28, 8728–8742. doi:10.1175/JCLI-D-15-0205.1.

Heikenfeld, M., White, B., Labbouz, L., and Stier, P. (2019). Aerosol effects on deep convection: The propagation of aerosol perturbations through convective cloud microphysics. *Atmos. Chem. Phys.* 19, 2601–2627. doi:10.5194/acp-19-2601-2019.

Henderson, G. R., Peings, Y., Furtado, J. C., and Kushner, P. J. (2018). Snow–atmosphere coupling in the Northern Hemisphere. *Nat. Clim. Chang.* 8, 954–963. doi:10.1038/s41558-018-0295-6.

Hock, R., Rasul, G., Adler, C., and et al (2019). "High Mountain Areas," in *Special Report on the Ocean and Cryosphere in a Changing Climate* Available at: https://report.ipcc.ch/srocc/pdf/SROCC_FinalDraft_Chapter2.pdf.

Hodnebrog, Ø., Myhre, G., Forster, P. M., Sillmann, J., and Samset, B. H. (2016). Local biomass burning is a dominant cause of the observed precipitation reduction in southern Africa. *Nat. Commun.* 7, 11236. doi:10.1038/ncomms11236.

Hodnebrog, Ø., Myhre, G., Samset, B. H., Alterskjær, K., Andrews, T., Boucher, O., et al. (2019). Water vapour adjustments and responses differ between climate drivers. *Atmos. Chem. Phys.* 19, 1–17. doi:10.5194/acp-2019-121.

Hoegh-Guldberg, O., Jacob, D., Taylor, M., Bindi, M., Brown, S., Camilloni, I., et al. (2019). "Impacts of 1.5ºC global warming on natural and human systems," in *IPCC Special Report on the impacts of global warming of 1.5°C above pre-industrial levels and related global greenhouse gas emission pathways, in the context of strengthening the global response to the threat of climate change.*, eds. V. Masson-Delmotte, P. Zhai, H.-O. Pörtner, D. Roberts, J. Skea, P. R. Shukla, et al. (Cambridge, United Kingdom and New York, NY, USA: Cambridge University Press), 175–311. Available at: https://www.ipcc.ch/sr15/chapter/chapter-3/.

Hoskins, B., and Woollings, T. (2015). Persistent extratropical regimes and climate extremes. *Curr. Clim. Chang. Reports* 1, 115–124. doi:10.1007/s40641-015-0020-8.

Hwang, Y. T., Frierson, D. M. W., and Kang, S. M. (2013). Anthropogenic sulfate aerosol and the southward shift of tropical precipitation in the late 20th century. *Geophys. Res. Lett.* 40, 2845–2850. doi:10.1002/grl.50502.

Jiang, P., Wang, D., and Cao, Y. (2016). Spatiotemporal characteristics of precipitation concentration and their possible links to urban extent in China. *Theor. Appl. Climatol.* 123, 757–768. doi:10.1007/s00704-015-1393-2.

Kageyama, M., Merkel, U., Otto-Bliesner, B., Prange, M., Abe-Ouchi, A., Lohmann, G., et al. (2013). Climatic impacts of fresh water hosing under last glacial Maximum conditions: A multi-model study. *Clim. Past* 9, 935–953. doi:10.5194/cp-9-935-2013.

Kao, A., Jiang, X., Li, L., Su, H., and Yung, Y. (2017). Precipitation, circulation, and cloud variability over the past two decades. *Earth Sp. Sci.* 4, 597–606. doi:10.1002/2017EA000319.

Karmakar, N., Chakraborty, A., and Nanjundiah, R. S. (2017). Increased sporadic extremes decrease the intraseasonal variability in the Indian summer monsoon rainfall. *Sci. Rep.* 7, 7824. doi:10.1038/s41598-017-07529-6.

Kendon, E. J., Stratton, R. A., Tucker, S., Marsham, J. H., Berthou, S., Rowell, D. P., et al. (2019). Enhanced future changes in wet and dry extremes over Africa at convection-permitting scale. *Nat. Commun.* 10, 1794. doi:10.1038/s41467-019-09776-9.

Khain, A., Lynn, B., Atmospheric, J. D.-J. of the, and 2010, U. (2010). Aerosol effects on intensity of landfalling hurricanes as seen from simulations with the WRF model with spectral bin microphysics. *journals.ametsoc.org*.

Konwar, M., Maheskumar, R. S., Kulkarni, J. R., Freud, E., Goswami, B. N., and Rosenfeld, D. (2012). Aerosol control on depth of warm rain in convective clouds. *J. Geophys. Res. Atmos.* 117.

Kooperman, G. J., Chen, Y., Hoffman, F. M., Koven, C. D., Lindsay, K., Pritchard, M. S., et al. (2018a). Forest response to rising CO2 drives zonally asymmetric rainfall change over tropical land. *Nat. Clim. Chang.* 8, 434–440. doi:10.1038/s41558-018-0144-7.

Kooperman, G. J., Fowler, M. D., Hoffman, F. M., Koven, C. D., Lindsay, K., Pritchard, M. S., et al. (2018b). Plant Physiological Responses to Rising CO 2 Modify Simulated Daily Runoff Intensity With Implications for Global-Scale Flood Risk Assessment. *Geophys. Res. Lett.* 45. doi:10.1029/2018GL079901.

Koren, I., Martins, J. V., Remer, L. A., and Afargan, H. (2008). Smoke invigoration versus inhibition of clouds over the Amazon. *Science* 321, 946–9. doi:10.1126/science.1159185.

Kossin, J. P. (2018). A global slowdown of tropical-cyclone translation speed. *Nature* 558, 104–107. doi:10.1038/s41586-018-0158-3.

Kuhlbrodt, T., Jones, C. G., Sellar, A., Storkey, D., Blockley, E., Stringer, M., et al. (2018). The Low-Resolution Version of HadGEM3 GC3.1: Development and Evaluation for Global Climate. *J. Adv. Model. Earth Syst.* 10, 2865–2888. doi:10.1029/2018MS001370.

Kumar, S., Allan, R. P., Zwiers, F., Lawrence, D. M., and Dirmeyer, P. A. (2015). Revisiting trends in wetness and dryness in the presence of internal climate variability and water limitations over land. *Geophys. Res. Lett.* doi:10.1002/2015GL066858.

Kumar, S., Newman, M., Wang, Y., and Livneh, B. (2019). Potential reemergence of seasonal soil moisture anomalies in North America. *J. Clim.* 32, 2707–2734. doi:10.1175/jcli-d-18-0540.1.

Kuo, C. C., Gan, T. Y., and Gizaw, M. (2015). Potential impact of climate change on intensity duration frequency curves of central Alberta. *Clim. Change* 130, 115–129. doi:10.1007/s10584-015-1347-9.

L'Heureux, M. L., Lee, S., and Lyon, B. (2013). Recent multidecadal strengthening of the Walker circulation across the tropical Pacific. *Nat. Clim. Chang.* 3, 571–576. doi:10.1038/nclimate1840.

Laîné, A., Nakamura, H., Nishii, K., and Miyasaka, T. (2014). A diagnostic study of future evaporation changes projected in CMIP5 climate models. *Clim. Dyn.* 42, 2745–2761. doi:10.1007/s00382-014-2087-7.

Lambert, F. H., Ferraro, A. J., and Chadwick, R. (2017). Land-ocean shifts in tropical precipitation linked to surface temperature and humidity change. *J. Clim.* 30, 4527–4545. doi:10.1175/JCLI-D-16-0649.1.

Lan, C. W., Lo, M. H., Chen, C. A., and Yu, J. Y. (2019). The mechanisms behind changes in the seasonality of global precipitation found in reanalysis products and CMIP5 simulations. *Clim. Dyn.* 53, 4173–4187. doi:10.1007/s00382-019-04781-6.

Lanzante, J. R. (2019). Uncertainties in tropical-cyclone translation speed. *Nature* 570, E6–E15. doi:10.1038/s41586-019-1223-2.

Lau, W. K. M., and Kim, K.-M. (2015). Robust Hadley Circulation changes and increasing global dryness due to CO2 warming from CMIP5 model projections. *Proc. Natl. Acad. Sci. U. S. A.* 112, 3630–5. doi:10.1073/pnas.1418682112.

Lavers, D. A., Allan, R. P., Villarini, G., Lloyd-Hughes, B., Brayshaw, D. J., and Wade, A. J. (2013). Future changes in atmospheric rivers and their implications for winter flooding in Britain. *Environ. Res. Lett.* 8. doi:10.1088/1748-9326/8/3/034010.

Lavers, D. A., Allan, R. P., Wood, E. F., Villarini, G., Brayshaw, D. J., and Wade, A. J. (2011). Winter floods in Britain are connected to atmospheric rivers. *Geophys. Res. Lett.* 38. doi:10.1029/2011GL049783.

Lawrence, D., and Vandecar, K. (2015). Effects of tropical deforestation on climate and agriculture. *Nat. Clim. Chang.* 5, 27–36. doi:10.1038/nclimate2430.

Lei, Y., Yao, T., Yang, K., Sheng, Y., Kleinherenbrink, M., Yi, S., et al. (2017). Lake seasonality across the Tibetan Plateau and their varying relationship with regional mass changes and local hydrology. *Geophys. Res. Lett.* 44, 892–900. doi:10.1002/2016GL072062.

Lejeune, Q., Davin, E. L., Guillod, B. P., and Seneviratne, S. I. (2015). Influence of Amazonian deforestation on the future evolution of regional surface fluxes, circulation, surface temperature and precipitation. *Clim. Dyn.* 44, 2769–2786. doi:10.1007/s00382-014-2203-8.

Lemordant, L., Gentine, P., Swann, A. S., Cook, B. I., and Scheff, J. (2018). Critical impact of vegetation physiology on the continental hydrologic cycle in response to increasing CO 2. *Proc. Natl. Acad. Sci.* 0, 201720712. doi:10.1073/pnas.1720712115.

Lenderink, G., Barbero, R., Loriaux, J. M., and Fowler, H. J. (2017). Super-Clausius-Clapeyron scaling of extreme hourly convective precipitation and its relation to large-scale atmospheric conditions. *J. Clim.* 30, 6037–6052. doi:10.1175/JCLI-D-16-0808.1.

Lenggenhager, S., Croci-Maspoli, M., Brönnimann, S., and Martius, O. (2018). On the dynamical coupling between atmospheric blocks and heavy precipitation events: A discussion of the southern Alpine flood in October 2000. *Q. J. R. Meteorol. Soc.* doi:10.1002/qj.3449.

Levy, M. C., Lopes, A. V., Cohn, A., Larsen, L. G., and Thompson, S. E. (2018). Land Use Change Increases Streamflow Across the Arc of Deforestation in Brazil. *Geophys. Res. Lett.* 45, 3520–3530. doi:10.1002/2017GL076526.

Li, G., Harrison, S. P., Bartlein, P. J., Izumi, K., and Colin Prentice, I. (2013). Precipitation scaling with temperature in warm and cold climates: An analysis of CMIP5 simulations. *Geophys. Res. Lett.* 40, 4018–4024. doi:10.1002/grl.50730.

Li, J., Xie, S.-P., Cook, E. R., Chen, F., Shi, J., Zhang, D. D., et al. (2018). Deciphering human contributions to Yellow River flow reductions and downstream drying using centuries-long tree ring records. *Geophys. Res. Lett.* doi:10.1029/2018GL081090.

Li, X., and Ting, M. (2017). Understanding the Asian summer monsoon response to greenhouse warming: the relative roles of direct radiative forcing and sea surface temperature change. *Clim. Dyn.* 49, 2863–2880. doi:10.1007/s00382-016-3470-3.

Li, Z., Lau, W. K. M., Ramanathan, V., Wu, G., Ding, Y., Manoj, M. G., et al. (2016). Aerosol and monsoon climate interactions over Asia. *Rev. Geophys.* 54, 866–929. doi:10.1002/2015RG000500.

Lin, L., Wang, Z., Xu, Y., Fu, Q., and Dong, W. (2018). Larger Sensitivity of Precipitation Extremes to Aerosol Than Greenhouse Gas Forcing in CMIP5 Models. *J. Geophys. Res. Atmos.* 123, 8062–8073. doi:10.1029/2018JD028821.

Little, K., Kingston, D. G., Cullen, N. J., and Gibson, P. B. (2019). The Role of Atmospheric Rivers for Extreme Ablation and Snowfall Events in the Southern Alps of New Zealand. *Geophys. Res. Lett.* doi:10.1029/2018GL081669.

Liu, C., and Allan, R. P. (2013). Observed and simulated precipitation responses in wet and dry regions 1850-2100. *Environ. Res. Lett.* doi:10.1088/1748-9326/8/3/034002.

Liu, F., Zhao, T., Wang, B., Liu, J., and Luo, W. (2018a). Different Global Precipitation Responses to Solar, Volcanic, and Greenhouse Gas Forcings. *J. Geophys. Res. Atmos.* 123, 4060–4072. doi:10.1029/2017JD027391.

Liu, H., Guo, J., Koren, I., Altaratz, O., Dagan, G., Wang, Y., et al. (2019). Non-Monotonic Aerosol Effect on Precipitation in Convective Clouds over Tropical Oceans. *Sci. Rep.* 9, 7809. doi:10.1038/s41598-019-44284-2.

Liu, L., Shawki, D., Voulgarakis, A., Kasoar, M., Samset, B. H., Myhre, G., et al. (2018b). A PDRMIP Multimodel study on the impacts of regional aerosol forcings on global and regional precipitation. *J. Clim.* 31, 4429–4447. doi:10.1175/JCLI-D-17-0439.1.

Loeb, N. G., Wang, H., Cheng, A., Kato, S., Fasullo, J. T., Xu, K. M., et al. (2016). Observational constraints on atmospheric and oceanic cross-equatorial heat transports: revisiting the precipitation asymmetry problem in climate models. *Clim. Dyn.* 46, 3239–3257. doi:10.1007/s00382-015-2766-z.

Lora, J. M. (2018). Components and mechanisms of hydrologic cycle changes over North America at the Last Glacial Maximum. *J. Clim.* 31, 7035–7051. doi:10.1175/JCLI-D-17-0544.1.

Loriaux, J. M., Lenderink, G., and Pier Siebesma, A. (2017). Large-scale controls on extreme precipitation. *J. Clim.* 30, 955–968. doi:10.1175/JCLI-D-16-0381.1.

Ma, J., Chadwick, R., Seo, K.-H., Dong, C., Huang, G., Foltz, G. R., et al. (2018). Responses of the Tropical Atmospheric Circulation to Climate Change and Connection to the Hydrological Cycle. *Annu. Rev. Earth Planet. Sci.* 46, 549–580. doi:10.1146/annurev-earth-082517-010102.

MacIntosh, C. R., Allan, R. P., Baker, L. H., Bellouin, N., Collins, W., Mousavi, Z., et al. (2016). Contrasting fast precipitation responses to tropospheric and stratospheric ozone forcing. *Geophys. Res. Lett.* 43, 1263–1271. doi:10.1002/2015GL067231.

Mankin, J. S., Seager, R., Smerdon, J. E., Cook, B. I., and Williams, A. P. (2019). Mid-latitude freshwater availability reduced by projected vegetation responses to climate change. *Nat. Geosci.* 12, 983–988. doi:10.1038/s41561-019-0480-x.

Mankin, J. S., Seager, R., Smerdon, J. E., Cook, B. I., Williams, A. P., and Horton, R. M. (2018). Blue Water Trade-Offs With Vegetation in a CO2-Enriched Climate. *Geophys. Res. Lett.* 45, 3115–3125. doi:10.1002/2018GL077051.

Marvel, K., Cook, B. I., Bonfils, C. J. W., Durack, P. J., Smerdon, J. E., and Williams, A. P. (2019). Twentieth-century hydroclimate changes consistent with human influence. *Nature* 569, 59–65. doi:10.1038/s41586-019-1149-8.

Mattingly, K. S., Mote, T. L., and Fettweis, X. (2018). Atmospheric River Impacts on Greenland Ice Sheet Surface Mass Balance. *J. Geophys. Res. Atmos.* 123, 8538–8560. doi:10.1029/2018JD028714.

McColl, K. A., Alemohammad, S. H., Akbar, R., Konings, A. G., Yueh, S., and Entekhabi, D. (2017). The global distribution and dynamics of surface soil moisture. *Nat. Geosci.* 10, 100–104. doi:10.1038/ngeo2868.

McGee, D., Donohoe, A., Marshall, J., and Ferreira, D. (2014). Changes in ITCZ location and cross-equatorial heat transport at the Last Glacial Maximum, Heinrich Stadial 1, and the mid-Holocene. *Earth Planet. Sci. Lett.* doi:10.1016/j.epsl.2013.12.043.

Meredith, E. P., Ulbrich, U., and Rust, H. W. (2019). The diurnal nature of future extreme precipitation intensification. *Geophys. Res. Lett.*, 2019GL082385. doi:10.1029/2019GL082385.

Merlis, T. M. (2015). Direct weakening of tropical circulations from masked CO 2 radiative forcing . *Proc. Natl. Acad. Sci.* doi:10.1073/pnas.1508268112.

Miller, P. W., Kumar, A., Mote, T. L., Moraes, F. D. S., and Mishra, D. R. (2019). Persistent Hydrological

Consequences of Hurricane Maria in Puerto Rico. *Geophys. Res. Lett.* doi:10.1029/2018GL081591.

Milly, P. C. D., and Dunne, K. A. (2016). Potential evapotranspiration and continental drying. *Nat. Clim. Chang.* 6, 946–949. doi:10.1038/nclimate3046.

Molnar, P., Fatichi, S., Gaál, L., Szolgay, J., and Burlando, P. (2015). Storm type effects on super Clausius-Clapeyron scaling of intense rainstorm properties with air temperature. *Hydrol. Earth Syst. Sci.* 19, 1753–1766. doi:10.5194/hess-19-1753-2015.

Moon, H., Guillod, B. P., Gudmundsson, L., and Seneviratne, S. I. (2019a). Soil moisture effects on afternoon precipitation occurrence in current climate models. *Geophys. Res. Lett.* doi:10.1029/2018GL080879.

Moon, I. J., Kim, S. H., and Chan, J. C. L. (2019b). Climate change and tropical cyclone trend. *Nature* 570, E3–E5. doi:10.1038/s41586-019-1222-3.

Morice, C. P., Kennedy, J. J., Rayner, N. A., and Jones, P. D. (2012). Quantifying uncertainties in global and regional temperature change using an ensemble of observational estimates: The HadCRUT4 data set. *J. Geophys. Res. Atmos.* 117. doi:10.1029/2011JD017187.

Morrill, C., Lowry, D. P., and Hoell, A. (2018). Thermodynamic and Dynamic Causes of Pluvial Conditions During the Last Glacial Maximum in Western North America. *Geophys. Res. Lett.* 45, 335–345. doi:10.1002/2017GL075807.

Muchan, K., Lewis, M., Hannaford, J., and Parry, S. (2015). The winter storms of 2013/2014 in the UK: hydrological responses and impacts. *Weather* 70, 55–61. doi:10.1002/wea.2469.

Musselman, K. N., Clark, M. P., Liu, C., Ikeda, K., and Rasmussen, R. (2017). Slower snowmelt in a warmer world. *Nat. Clim. Chang.* 7, 214–219. doi:10.1038/nclimate3225.

Musselman, K. N., Lehner, F., Ikeda, K., Clark, M. P., Prein, A. F., Liu, C., et al. (2018). Projected increases and shifts in rain-on-snow flood risk over western North America. *Nat. Clim. Chang.* 8, 808–812. doi:10.1038/s41558-018-0236-4.

Myhre, G., Alterskjær, K., Stjern, C. W., Hodnebrog, Ø., Marelle, L., Samset, B. H., et al. (2019). Frequency of extreme precipitation increases extensively with event rareness under global warming. *Sci. Rep.* 9, 16063. doi:10.1038/s41598-019-52277-4.

Myhre, G., Samset, B. H., Hodnebrog, O., Andrews, T., Boucher, O., Faluvegi, G., et al. (2018). Sensible heat has significantly affected the global hydrological cycle over the historical period. *Nat. Commun.* 9. doi:10.1038/s41467-018-04307-4.

Neelin, J. D., Sahany, S., Stechmann, S. N., and Bernstein, D. N. (2017). Global warming precipitation accumulation increases above the current-climate cutoff scale. *Proc. Natl. Acad. Sci.* 114, 1258–1263. doi:10.1073/pnas.1615333114.

Nie, J., Sobel, A. H., Shaevitz, D. A., and Wang, S. (2018). Dynamic amplification of extreme precipitation sensitivity. *Proc. Natl. Acad. Sci.*, 201800357. doi:10.1073/pnas.1800357115.

Nikumbh, A., Chakraborty, A., and Bhat, G. S. (2019). Recent spatial aggregation tendency of rainfall extremes over India. *Sci. Rep.* 9, 1–29. doi:10.1038/s41598-019-46719-2.

O'Gorman, P. A. (2014). Contrasting responses of mean and extreme snowfall to climate change. *Nature* 512, 416–418. doi:10.1038/nature13625.

O'Gorman, P. A. (2015). Precipitation Extremes Under Climate Change. *Curr. Clim. Chang. Reports* 1, 49–59. doi:10.1007/s40641-015-0009-3.

O'Gorman, P. A., Allan, R. P., Byrne, M. P., and Previdi, M. (2012). Energetic Constraints on Precipitation Under Climate Change. *Surv. Geophys.* 33, 585–608. doi:10.1007/s10712-011-9159-6.

Oltmanns, M., Straneo, F., and Tedesco, M. (2018). Increased Greenland melt triggered by large-scale, year-round precipitation events. *Cryosph. Discuss.* 13, 1–18. doi:10.5194/tc-2018-243.

Oster, J. L., Ibarra, D. E., Winnick, M. J., and Maher, K. (2015). Steering of westerly storms over western North America at the Last Glacial Maximum. *Nat. Geosci.* doi:10.1038/ngeo2365.

Pall, P., Tallaksen, L. M., and Stordal, F. (2019). A Climatology of Rain-on-Snow Events for Norway. *J. Clim.* 32, 6995–7016. doi:10.1175/jcli-d-18-0529.1.

Paltan, H., Waliser, D., Lim, W. H., Guan, B., Yamazaki, D., Pant, R., et al. (2017). Global Floods and Water Availability Driven by Atmospheric Rivers. *Geophys. Res. Lett.* 44, 10,387-10,395. doi:10.1002/2017GL074882.

Parsons, L. A., Yin, J., Overpeck, J. T., Stouffer, R. J., and Malyshev, S. (2014). Influence of the atlantic meridional overturning circulation on the monsoon rainfall and carbon balance of the American tropics.

Geophys. Res. Lett. doi:10.1002/2013GL058454.

Pathirana, A., Denekew, H. B., Veerbeek, W., Zevenbergen, C., and Banda, A. T. (2014). Impact of urban growth-driven landuse change on microclimate and extreme precipitation - A sensitivity study. *Atmos. Res.* doi:10.1016/j.atmosres.2013.10.005.

Patil, N., Venkataraman, C., Muduchuru, K., Ghosh, S., and Mondal, A. (2018). Disentangling sea-surface temperature and anthropogenic aerosol influences on recent trends in South Asian monsoon rainfall. *Clim. Dyn.*, 1–16. doi:10.1007/s00382-018-4251-y.

Pederson, N., Hessl, A. E., Baatarbileg, N., Anchukaitis, K. J., and Di Cosmo, N. (2014). Pluvials, droughts, the Mongol Empire, and modern Mongolia. *Proc. Natl. Acad. Sci.* doi:10.1073/pnas.1318677111.

Pei, L., Moore, N., Zhong, S., Kendall, A. D., Gao, Z., and Hyndman, D. W. (2016). Effects of irrigation on summer precipitation over the United States. *J. Clim.* 29, 3541–3558. doi:10.1175/JCLI-D-15-0337.1.

Pendergrass, A. G. (2018). What precipitation is extreme? *Science (80-.).* 360, 1072–1073. doi:10.1126/science.aat1871.

Pendergrass, A. G., and Hartmann, D. L. (2014a). The atmospheric energy constraint on global-mean precipitation change. *J. Clim.* 27, 757–768. doi:10.1175/JCLI-D-13-00163.1.

Pendergrass, A. G., and Hartmann, D. L. (2014b). Two modes of change of the distribution of rain. *J. Clim.* 27, 8357–8371. doi:10.1175/JCLI-D-14-00182.1.

Pendergrass, A. G., Reed, K. A., and Medeiros, B. (2016). The link between extreme precipitation and convective organization in a warming climate: Global radiative-convective equilibrium simulations. *Geophys. Res. Lett.* 43, 11,445-11,452. doi:10.1002/2016GL071285.

Persad, G. G., Paynter, D. J., Ming, Y., and Ramaswamy, V. (2017). Competing atmospheric and surface-driven impacts of absorbing aerosols on the East Asian summertime climate. *J. Clim.* 30, 8929–8949. doi:10.1175/JCLI-D-16-0860.1.

Peters, W., van der Velde, I. R., van Schaik, E., Miller, J. B., Ciais, P., Duarte, H. F., et al. (2018). Increased water-use efficiency and reduced CO2 uptake by plants during droughts at a continental scale. *Nat. Geosci.*, 11–16. doi:10.1038/s41561-018-0212-7.

Pfahl, S., O’Gorman, P. A., and Fischer, E. M. (2017). Understanding the regional pattern of projected future changes in extreme precipitation. *Nat. Clim. Chang.* 7, 423–427. doi:10.1038/nclimate3287.

Pfleiderer, P., Schleussner, C., and Coumou, D. (2018). Boreal summer weather becomes more persistent in a warmer world. *Nat. Clim. Chang.* 9, 666–671. doi:10.1038/s41558-019-0555-0.

Phibbs, S., and Toumi, R. (2016). The dependence of precipitation and its footprint on atmospheric temperature in idealized extratropical cyclones. *J. Geophys. Res.* 121, 8743–8754. doi:10.1002/2015JD024286.

Plesca, E., Buehler, S. A., and Grützun, V. (2018). The fast response of the tropical circulation to CO2 forcing. *J. Clim.*, JCLI-D-18-0086.1. doi:10.1175/JCLI-D-18-0086.1.

Polson, D., Bollasina, M., Hegerl, G. C., and Wilcox, L. J. (2014). Decreased monsoon precipitation in the Northern Hemisphere due to anthropogenic aerosols. *Geophys. Res. Lett.* 41, 6023–6029. doi:10.1002/2014GL060811.

Polson, D., and Hegerl, G. C. (2017). Strengthening contrast between precipitation in tropical wet and dry regions. *Geophys. Res. Lett.* 44, 365–373. doi:10.1002/2016GL071194.

Popp, M., and Silvers, L. G. (2017). Double and single ITCZs with and without clouds. *J. Clim.* doi:10.1175/JCLI-D-17-0062.1.

Prein, A. F., Rasmussen, R. M., Ikeda, K., Liu, C., Clark, M. P., and Holland, G. J. (2017). The future intensification of hourly precipitation extremes. *Nat. Clim. Chang.* 7, 48–52. doi:10.1038/nclimate3168.

Qian, Y., Gong, D., Fan, J., Leung, L. R., Bennartz, R., Chen, D., et al. (2009). Heavy pollution suppresses light rain in China: Observations and modeling. *J. Geophys. Res.* 114, D00K02. doi:10.1029/2008JD011575.

Qu, Y., Chen, B., Ming, J., Lynn, B. H., and Yang, M.-J. (2017). Aerosol Impacts on the Structure, Intensity, and Precipitation of the Landfalling Typhoon Saomai (2006). *J. Geophys. Res. Atmos.* 122, 11,825-11,842. doi:10.1002/2017JD027151.

Ralph, F. M., Dettinger, M. C. L. D., Cairns, M. M., Galarneau, T. J., and Eylander, J. (2018). Defining “Atmospheric river" : How the glossary of meteorology helped resolve a debate. *Bull. Am. Meteorol. Soc.* 99, 837–839. doi:10.1175/BAMS-D-17-0157.1.

Ramos, A. M., Tomé, R., Trigo, R. M., Liberato, M. L. R., and Pinto, J. G. (2016). Projected changes in atmospheric rivers affecting Europe in CMIP5 models. *Geophys. Res. Lett.* 43, 9315–9323. doi:10.1002/2016GL070634.

Rauber, R. M., Geerts, B., Xue, L., French, J., Friedrich, K., Rasmussen, R. M., et al. (2019). Wintertime Orographic Cloud Seeding—A Review. *J. Appl. Meteorol. Climatol.* 58, 2117–2140. doi:10.1175/JAMC-D-18-0341.1.

Rhoades, A. M., Jones, A. D., and Ullrich, P. A. (2018). The Changing Character of the California Sierra Nevada as a Natural Reservoir. *Geophys. Res. Lett.* 45, 8-13,13,19. doi:10.1029/2018GL080308.

Richardson, T. B., Forster, P., Andrews, T., Boucher, O., Faluvegi, G., Fläschner, D., et al. (2018a). Drivers of precipitation change: An energetic understanding. *J. Clim.* 31, 9641–9657. doi:10.1175/JCLI-D-17-0240.1.

Richardson, T. B., Forster, P. M., Andrews, T., Boucher, O., Faluvegi, G., Fläschner, D., et al. (2018b). Carbon Dioxide Physiological Forcing Dominates Projected Eastern Amazonian Drying. *Geophys. Res. Lett.* doi:10.1002/2017GL076520.

Richardson, T. B., Forster, P. M., Andrews, T., and Parker, D. J. (2016). Understanding the rapid precipitation response to CO 2 and aerosol forcing on a regional scale. *J. Clim.* 29, 583–594. doi:10.1175/JCLI-D-15-0174.1.

Rodell, M., Beaudoing, H. K., L'Ecuyer, T. S., Olson, W. S., Famiglietti, J. S., Houser, P. R., et al. (2015). The observed state of the water cycle in the early twenty-first century. *J. Clim.* 28, 8289–8318. doi:10.1175/JCLI-D-14-00555.1.

Roderick, M. L., Sun, F., Lim, W. H., and Farquhar, G. D. (2014). A general framework for understanding the response of the water cycle to global warming over land and ocean. *Hydrol. Earth Syst. Sci.* 18, 1575–1589. doi:10.5194/hess-18-1575-2014.

Romps, D. M. (2016). Clausius–Clapeyron Scaling of CAPE from Analytical Solutions to RCE. *J. Atmos. Sci.* doi:10.1175/jas-d-15-0327.1.

Rosenfeld, D., Clavner, M., and Nirel, R. (2011). Pollution and dust aerosols modulating tropical cyclones intensities. *Atmos. Res.* 102. doi:10.1016/j.atmosres.2011.06.006.

Rosenfeld, D., Lohmann, U., Raga, G. B., O'dowd, C. D., Kulmala, M., Fuzzi, S., et al. (2008). Flood or drought: How do aerosols affect precipitation? *Science (80-.).* 321, 1309–1313.

Rosenfeld, D., Woodley, W. L., Khain, A., Cotton, W. R., Carrió, G., Ginis, I., et al. (2012). Aerosol effects on microstructure and intensity of tropical cyclones. *Bull. Am. Meteorol. Soc.* 93. doi:10.1175/BAMS-D-11-00147.1.

Rotstayn, L. D., Collier, M. A., and Luo, J. -j. (2015). Effects of declining aerosols on projections of zonally averaged tropical precipitation. *Environ. Res. Lett.* 10. doi:10.1088/1748-9326/10/4/044018.

Routson, C. C., McKay, N. P., Kaufman, D. S., Erb, M. P., Goosse, H., Shuman, B. N., et al. (2019). Mid-latitude net precipitation decreased with Arctic warming during the Holocene. *Nature* 568, 83–87. doi:10.1038/s41586-019-1060-3.

Roxy, M. K., Ghosh, S., Pathak, A., Athulya, R., Mujumdar, M., Murtugudde, R., et al. (2017). A threefold rise in widespread extreme rain events over central India. *Nat. Commun.* 8. doi:10.1038/s41467-017-00744-9.

Salzmann, M. (2016). Global warming without global mean precipitation increase'. *Sci. Adv.* 2, e1501572--e1501572. doi:10.1126/sciadv.1501572.

Samanta, D., Karnauskas, K. B., and Goodkin, N. F. (2019). Tropical Pacific SST and ITCZ Biases in Climate Models: Double Trouble for Future Rainfall Projections? *Geophys. Res. Lett.* doi:10.1029/2018GL081363.

Samset, B. H., Myhre, G., Forster, P. M., Hodnebrog, Andrews, T., Faluvegi, G., et al. (2016). Fast and slow precipitation responses to individual climate forcers: A PDRMIP multimodel study. *Geophys. Res. Lett.* 43, 2782–2791. doi:10.1002/2016GL068064.

Samset, B. H., Myhre, G., Forster, P. M., Hodnebrog, Ø., Andrews, T., Boucher, O., et al. (2018a). Weak hydrological sensitivity to temperature change over land, independent of climate forcing. *npj Clim. Atmos. Sci.* 1, 3. doi:10.1038/s41612-017-0005-5.

Samset, B. H., Sand, M., Smith, C. J., Bauer, S. E., Forster, P. M., Fuglestvedt, J. S., et al. (2018b). Climate Impacts From a Removal of Anthropogenic Aerosol Emissions. *Geophys. Res. Lett.* 45, 1020–1029. doi:10.1002/2017GL076079.

Sandvik, M. I., Sorteberg, A., and Rasmussen, R. (2018). Sensitivity of historical orographically enhanced extreme precipitation events to idealized temperature perturbations. *Clim. Dyn.* 50, 143–157. doi:10.1007/s00382-017-3593-1.

Sarangi, C., Tripathi, S. N., Qian, Y., Kumar, S., and Ruby Leung, L. (2018). Aerosol and Urban Land Use Effect on Rainfall Around Cities in Indo-Gangetic Basin From Observations and Cloud Resolving Model Simulations. *J. Geophys. Res. Atmos.* 123, 3645–3667. doi:10.1002/2017JD028004.

Scheff, J., and Frierson, D. M. W. (2014). Scaling potential evapotranspiration with greenhouse warming. *J. Clim.* 27, 1539–1558. doi:10.1175/JCLI-D-13-00233.1.

Scheff, J., and Frierson, D. M. W. (2015). Terrestrial aridity and its response to greenhouse warming across CMIP5 climate models. *J. Clim.* 28, 5583–5600. doi:10.1175/JCLI-D-14-00480.1.

Scheff, J., Seager, R., Liu, H., and Coats, S. (2017). Are glacials dry? Consequences for paleoclimatology and for greenhouse warming. *J. Clim.* doi:10.1175/JCLI-D-16-0854.1.

Schmid, P. E., and Niyogi, D. (2017). Modeling urban precipitation modification by spatially heterogeneous aerosols. *J. Appl. Meteorol. Climatol.* 56, 2141–2153. doi:10.1175/JAMC-D-16-0320.1.

Schwarz, M., Folini, D., Yang, S., Allan, R. P., and Wild, M. (2020). Changes in atmospheric shortwave absorption as important driver of dimming and brightening. *Nat. Geosci. 2020 132* 13, 110–115. doi:10.1038/s41561-019-0528-y.

Scoccimarro, E., Villarini, G., Vichi, M., Zampieri, M., Fogli, P. G., Bellucci, A., et al. (2015). Projected changes in intense precipitation over Europe at the daily and subdaily time scales. *J. Clim.* 28, 6193–6203. doi:10.1175/JCLI-D-14-00779.1.

Séférian, R., Delire, C., Decharme, B., Voldoire, A., David Salas, Y. M., Chevallier, M., et al. (2016). Development and evaluation of CNRM Earth system model-CNRM-ESM1. *Geosci. Model Dev.* 9, 1423–1453. doi:10.5194/gmd-9-1423-2016.

Séférian, R., Nabat, P., Michou, M., Saint-Martin, D., Voldoire, A., Colin, J., et al. (2019). Evaluation of CNRM Earth-System model, CNRM-ESM 2-1: role of Earth system processes in present-day and future climate. *J. Adv. Model. Earth Syst.* n/a, 2019MS001791. doi:10.1029/2019MS001791.

Seth, A., Giannini, A., Rojas, M., Rauscher, S. A., Bordoni, S., Singh, D., et al. (2019). Monsoon Responses to Climate Changes—Connecting Past, Present and Future. *Curr. Clim. Chang. Reports* 5, 63–79. doi:10.1007/s40641-019-00125-y.

Sharma, S., Blagrave, K., O'Reilly, C. M., Samantha, O., Ryan, B., Magee, M., et al. (2019). Widespread loss of lake ice around the Northern Hemisphere in a warming world. Submitted. *Nat. Clim. Chang.* doi:10.1038/s41558-018-0393-5.

Shaw, T. A., and Tan, Z. (2018). Testing latitudinally-dependent explanations of the circulation response to increased CO2 using aquaplanet models. *Geophys. Res. Lett.* doi:10.1029/2018GL078974.

Sherwood, S. C., Bony, S., Boucher, O., Bretherton, C., Forster, P. M., Gregory, J. M., et al. (2015). Adjustments in the forcing-feedback framework for understanding climate change. *Bull. Am. Meteorol. Soc.* 96, 217–228. doi:10.1175/BAMS-D-13-00167.1.

Shine, K. P., Allan, R. P., Collins, W. J., and Fuglestvedt, J. S. (2015). Metrics for linking emissions of gases and aerosols to global precipitation changes. *Earth Syst. Dyn.* 6, 525–540. doi:10.5194/esd-6-525-2015.

Siler, N., Roe, G. H., Armour, K. C., and Feldl, N. (2018). Revisiting the surface-energy-flux perspective on the sensitivity of global precipitation to climate change. *Clim. Dyn.* doi:10.1007/s00382-018-4359-0.

Sillmann, J., Stjern, C. W., Myhre, G., Samset, B. H., Hodnebrog, Ø., Boucher, O., et al. (2019). Extreme wet and dry conditions affected differently by greenhouse gases and aerosols. *npj Clim. Atmos. Sci.* 2. doi:10.1038/s41612-019-0079-3.

Singarayer, J. S., Valdes, P. J., and Roberts, W. H. G. (2017). Ocean dominated expansion and contraction of the late Quaternary tropical rainbelt. *Sci. Rep.* 7. doi:10.1038/s41598-017-09816-8.

Singh, M. S., and O'Gorman, P. A. (2014). Influence of microphysics on the scaling of precipitation extremes with temperature. *Geophys. Res. Lett.* 41, 6037–6044. doi:10.1002/2014GL061222.

Skinner, C. B., Poulsen, C. J., Chadwick, R., Diffenbaugh, N. S., and Fiorella, R. P. (2017). The role of plant CO2 physiological forcing in shaping future daily-scale precipitation. *J. Clim.* 30, 2319–2340. doi:10.1175/JCLI-D-16-0603.1.

Skliris, N., Zika, J. D., Nurser, G., Josey, S. A., and Marsh, R. (2016). Global water cycle amplifying at less than the Clausius-Clapeyron rate. *Sci. Rep.* 6. doi:10.1038/srep38752.

Sohn, B. J., Yeh, S. W., Schmetz, J., and Song, H. J. (2013). Observational evidences of Walker circulation change over the last 30 years contrasting with GCM results. *Clim. Dyn.* 40, 1721–1732. doi:10.1007/s00382-012-1484-z.

Spracklen, D. V., and Garcia-Carreras, L. (2015). The impact of Amazonian deforestation on Amazon basin rainfall. *Geophys. Res. Lett.* 42, 9546–9552. doi:10.1002/2015GL066063.

Stephens, E., Day, J. J., Pappenberger, F., and Cloke, H. (2015a). Precipitation and floodiness. *Geophys. Res. Lett.* 42, 10316–10323. doi:10.1002/2015GL066779.

Stephens, G. L., Hakuba, M. Z., Webb, M. J., Lebsock, M., Yue, Q., Kahn, B. H., et al. (2018). Regional Intensification of the Tropical Hydrological Cycle During ENSO. *Geophys. Res. Lett.* 45, 4361–4370. doi:10.1029/2018GL077598.

Stephens, G. L., Li, J., Wild, M., Clayson, C. A., Loeb, N., Kato, S., et al. (2012). An update on Earth's energy balance in light of the latest global observations. *Nat. Geosci.* 5, 691–696. doi:10.1038/ngeo1580.

Stephens, G. L., O'Brien, D., Webster, P. J., Pilewski, P., Kato, S., and Li, J. L. (2015b). The albedo of earth. *Rev. Geophys.* 53, 141–163. doi:10.1002/2014RG000449.

Stjern, C. W., Samset, B. H., Myhre, G., Forster, P. M., Hodnebrog, Ø., Andrews, T., et al. (2017). Rapid Adjustments Cause Weak Surface Temperature Response to Increased Black Carbon Concentrations. *J. Geophys. Res. Atmos.* 122, 11,462-11,481. doi:10.1002/2017JD027326.

Su, H., Jiang, J. H., Neelin, J. D., Shen, T. J., Zhai, C., Yue, Q., et al. (2017). Tightening of tropical ascent and high clouds key to precipitation change in a warmer climate. *Nat. Commun.* 8, 15771. doi:10.1038/ncomms15771.

Su, H., Zhai, C., Jiang, J. H., Wu, L., Neelin, J. D., and Yung, Y. L. (2019). A dichotomy between model responses of tropical ascent and descent to surface warming. *npj Clim. Atmos. Sci.* 2, 8. doi:10.1038/s41612-019-0066-8.

Swann, A. L. S., Hoffman, F. M., Koven, C. D., and Randerson, J. T. (2016). Plant responses to increasing CO2 reduce estimates of climate impacts on drought severity. *Proc. Natl. Acad. Sci.* 113, 10019–10024. doi:10.1073/pnas.1604581113.

Swart, N. C., Cole, J. N. S., Kharin, V. V., Lazare, M., Scinocca, J. F., Gillett, N. P., et al. (2019). The Canadian Earth System Model version 5 (CanESM5.0.3). *Geosci. Model Dev. Discuss.* 12, 1–68. doi:10.5194/gmd-2019-177.

Takahashi, H. G., Fujinami, H., Yasunari, T., Matsumoto, J., and Baimoung, S. (2015). Role of tropical cyclones along the monsoon trough in the 2011 Thai flood and interannual variability. *J. Clim.* 28, 1465–1476. doi:10.1175/JCLI-D-14-00147.1.

Takahashi, H. G., and Polcher, J. (2019). Weakening of rainfall intensity on wet soils over the wet Asian monsoon region using a high-resolution regional climate model. *Prog. Earth Planet. Sci.* 6, 26. doi:10.1186/s40645-019-0272-3.

Talib, J., Woolnough, S. J., Klingaman, N. P., and Holloway, C. E. (2018). The Role of the Cloud Radiative Effect in the Sensitivity of the Intertropical Convergence Zone to Convective Mixing. *J. Clim.* 31, 6821–6838. doi:10.1175/JCLI-D-17-0794.1.

Tan, X., and Gan, T. Y. (2015). Contribution of human and climate change impacts to changes in streamflow of Canada. *Sci. Rep.* 5. doi:10.1038/srep17767.

Tan, X., Gan, T. Y., Chen, S., Horton, D. E., Chen, X., Liu, B., et al. (2019). Trends in persistent seasonal-scale atmospheric circulation patterns responsible for seasonal precipitation totals and occurrences of precipitation extremes over Canada. *J. Clim.* 32, 7105–7126. doi:10.1175/jcli-d-18-0408.1.

Tandon, N. F., Zhang, X., and Sobel, A. H. (2018). Understanding the Dynamics of Future Changes in Extreme Precipitation Intensity. *Geophys. Res. Lett.* 45, 2870–2878. doi:10.1002/2017GL076361.

Tang, Q., Zhang, X., and Francis, J. A. (2014). Extreme summer weather in northern mid-latitudes linked to a vanishing cryosphere. *Nat. Clim. Chang.* 4, 45–50. doi:10.1038/nclimate2065.

Tatebe, H., Ogura, T., Nitta, T., Komuro, Y., Ogochi, K., Takemura, T., et al. (2019). Description and basic evaluation of simulated mean state, internal variability, and climate sensitivity in MIROC6. *Geosci. Model Dev.* 12, 2727–2765. doi:10.5194/gmd-12-2727-2019.

Taylor, C. M. (2015). Detecting soil moisture impacts on convective initiation in Europe. *Geophys. Res. Lett.* 42, 4631–4638. doi:10.1002/2015GL064030.

Taylor, C. M., Belusic, D., Guichard, F., Parker, D. J., Vischel, T., Bock, O., et al. (2017). Frequency of extreme Sahelian storms tripled since 1982 in satellite observations. *Nature* 544, 475–478.

doi:10.1038/nature22069.
Taylor, C. M., Birch, C. E., Parker, D. J., Dixon, N., Guichard, F., Nikulin, G., et al. (2013). Modeling soil moisture-precipitation feedback in the Sahel: Importance of spatial scale versus convective parameterization. *Geophys. Res. Lett.* 40, 6213–6218. doi:10.1002/2013GL058511.
Thornton, J. A., Virts, K. S., Holzworth, R. H., and Mitchell, T. P. (2017). Lightning enhancement over major oceanic shipping lanes. *Geophys. Res. Lett.* 44, 9102–9111. doi:10.1002/2017GL074982.
Tian, D., Dong, W., Gong, D., Guo, Y., and Yang, S. (2017). Fast responses of climate system to carbon dioxide, aerosols and sulfate aerosols without the mediation of SST in the CMIP5. *Int. J. Climatol.* 37, 1156–1166. doi:10.1002/joc.4763.
Trenberth, K. E., Fasullo, J. T., and Mackaro, J. (2011). Atmospheric moisture transports from ocean to land and global energy flows in reanalyses. *J. Clim.* 24, 4907–4924. doi:10.1175/2011JCLI4171.1.
Turner, J., Phillips, T., Thamban, M., Rahaman, W., Marshall, G. J., Wille, J. D., et al. (2019). The Dominant Role of Extreme Precipitation Events in Antarctic Snowfall Variability. *Geophys. Res. Lett.* doi:10.1029/2018GL081517.
Ukkola, A. M., Prentice, I. C., Keenan, T. F., Van Dijk, A. I. J. M., Viney, N. R., Myneni, R. B., et al. (2016). Reduced streamflow in water-stressed climates consistent with CO2 effects on vegetation. *Nat. Clim. Chang.* doi:10.1038/nclimate2831.
Undorf, S., Polson, D., Bollasina, M. A., Ming, Y., Schurer, A., and Hegerl, G. C. (2018). Detectable Impact of Local and Remote Anthropogenic Aerosols on the 20th Century Changes of West African and South Asian Monsoon Precipitation. *J. Geophys. Res. Atmos.* 123, 4871–4889. doi:10.1029/2017JD027711.
Vallis, G. K., Zurita-Gotor, P., Cairns, C., and Kidston, J. (2015). Response of the large-scale structure of the atmosphere to global warming. *Q. J. R. Meteorol. Soc.* doi:10.1002/qj.2456.
van der Wiel, K., Wanders, N., Selten, F. M., and Bierkens, M. F. P. (2019). Added Value of Large Ensemble Simulations for Assessing Extreme River Discharge in a 2 °C Warmer World. *Geophys. Res. Lett.* 46, 2093–2102. doi:10.1029/2019GL081967.
Vanniere, B., Demory, M.-E., Vidale, P. L., Schiemann, R., Roberts, M. J., Roberts, C., et al. (2018). Multi-model evaluation of the sensitivity of the global energy budget and hydrological cycle to resolution. *Clim. Dyn. print*. doi:10.1007/s00382-018-4547-y.
Voldoire, A., Saint-Martin, D., Sénési, S., Decharme, B., Alias, A., Chevallier, M., et al. (2019). Evaluation of CMIP6 DECK Experiments With CNRM-CM6-1. *J. Adv. Model. Earth Syst.* 11, 2177–2213. doi:10.1029/2019MS001683.
Waliser, D., and Guan, B. (2017). Extreme winds and precipitation during landfall of atmospheric rivers. *Nat. Geosci.* 10, 179–183. doi:10.1038/ngeo2894.
Wang-Erlandsson, L., Fetzer, I., Keys, P. W., Van Der Ent, R. J., Savenije, H. H. G., and Gordon, L. J. (2018). Remote land use impacts on river flows through atmospheric teleconnections. *Hydrol. Earth Syst. Sci.* 22, 4311–4328. doi:10.5194/hess-22-4311-2018.
Wang, W., Lee, X., Xiao, W., Liu, S., Schultz, N., Wang, Y., et al. (2018). Global lake evaporation accelerated by changes in surface energy allocation in a warmer climate. *Nat. Geosci.* 11, 410–414. doi:10.1038/s41561-018-0114-8.
Wang, Y., Khalizov, A., Levy, M., and Zhang, R. (2013). New Directions: Light absorbing aerosols and their atmospheric impacts. *Atmos. Environ.* 81, 713–715. doi:10.1016/J.ATMOSENV.2013.09.034.
Wang, Y., Lee, K.-H., Lin, Y., Levy, M., and Zhang, R. (2014). Distinct effects of anthropogenic aerosols on tropical cyclones. *Nat. Clim. Chang.* 4, 368–373. doi:10.1038/nclimate2144.
Wasko, C., and Nathan, R. (2019). Influence of changes in rainfall and soil moisture on trends in flooding. *J. Hydrol.* 575, 432–441. doi:10.1016/j.jhydrol.2019.05.054.
Watanabe, M., Kamae, Y., Shiogama, H., DeAngelis, A. M., and Suzuki, K. (2018). Low clouds link equilibrium climate sensitivity to hydrological sensitivity. *Nat. Clim. Chang.*, 1. doi:10.1038/s41558-018-0272-0.
Watt-Meyer, O., and Frierson, D. M. W. (2019). ITCZ width controls on Hadley cell extent and eddy-driven jet position and their response to warming. *J. Clim.* 32, 1151–1166. doi:10.1175/JCLI-D-18-0434.1.
Watt-Meyer, O., Frierson, D. M. W., and Fu, Q. (2019). Hemispheric asymmetry of tropical expansion under CO 2 forcing. *Geophys. Res. Lett.*, 2019GL083695. doi:10.1029/2019GL083695.
Webb, M. J., Lock, A. P., and Lambert, F. H. (2018). Interactions between hydrological sensitivity, radiative cooling, stability, and low-level cloud amount feedback. *J. Clim.* 31, 1833–1850. doi:10.1175/JCLI-D-

16-0895.1.
Wentz, F. J., Ricciardulli, L., Hilburn, K., and Mears, C. (2007). How Much More Rain Will Global Warming Bring? *Science (80-.).* 317, 233–235. doi:10.1126/science.1140746.
Westra, S., Fowler, H. J., Evans, J. P., Alexander, L. V., Berg, P., Johnson, F., et al. (2014). Future changes to the intensity and frequency of short-duration extreme rainfall. *Rev. Geophys.* 52, 522–555. doi:10.1002/2014RG000464.
Wey, H. W., Lo, M. H., Lee, S. Y., Yu, J. Y., and Hsu, H. H. (2015). Potential impacts of wintertime soil moisture anomalies from agricultural irrigation at low latitudes on regional and global climates. *Geophys. Res. Lett.* 42, 8605–8614. doi:10.1002/2015GL065883.
Wilcox, L., Dunstone, N., Lewinschal, A., Bollasina, M., Ekman, A., and Highwood, E. (2018). Mechanisms for a remote response to Asian aerosol emissions in boreal winter. *Atmos. Chem. Phys. Discuss.* 19, 1–21. doi:10.5194/acp-2018-980.
Wilcox, L. J., Liu, Z., Samset, B. H., Hawkins, E., Lund, M. T., Nordling, K., et al. (2020). Accelerated increases in global and Asian summer monsoon precipitation from future aerosol reductions. *Atmos. Chem. Phys. Discuss.* 2020. doi:10.5194/acp-2019-1188.
Wild, M. (2012). Enlightening Global Dimming and Brightening. *Bull. Am. Meteorol. Soc.* 93, 27–37. doi:10.1175/BAMS-D-11-00074.1.
Wille, J. D., Favier, V., Dufour, A., Gorodetskaya, I. V, Turner, J., Agosta, C., et al. (2019). West Antarctic surface melt triggered by atmospheric rivers. *Nat. Geosci.* 12, 911–916. doi:10.1038/s41561-019-0460-1.
Willett, K. M., Dunn, R. J. H., Thorne, P. W., Bell, S., De Podesta, M., Parker, D. E., et al. (2014). HadISDH land surface multi-variable humidity and temperature record for climate monitoring. *Clim. Past* 10, 1983–2006. doi:10.5194/cp-10-1983-2014.
Willett, K. M., Jones, P. D., Gillett, N. P., and Thorne, P. W. (2008). Recent changes in surface humidity: Development of the HadCRUH dataset. *J. Clim.* 21, 5364–5383. doi:10.1175/2008JCLI2274.1.
Wills, R. C., Levine, X. J., and Schneider, T. (2017). Local energetic constraints on walker circulation strength. *J. Atmos. Sci.* 74, 1907–1922. doi:10.1175/JAS-D-16-0219.1.
Wodzicki, K. R., and Rapp, A. D. (2016). Long-term characterization of the Pacific ITCZ using TRMM, GPCP, and ERA-Interim. *J. Geophys. Res. Atmos.* 121, 3153–3170. doi:10.1002/2015JD024458.
Woldemeskel, F., and Sharma, A. (2016). Should flood regimes change in a warming climate? The role of antecedent moisture conditions. *Geophys. Res. Lett.* 43, 7556–7563. doi:10.1002/2016GL069448.
Woollings, T., Barriopedro, D., Methven, J., Son, S. W., Martius, O., Harvey, B., et al. (2018). Blocking and its Response to Climate Change. *Curr. Clim. Chang. Reports* 4, 287–300. doi:10.1007/s40641-018-0108-z.
Wu, T., Lu, Y., Fang, Y., Xin, X., Li, L., Li, W., et al. (2019). The Beijing Climate Center Climate System Model (BCC-CSM): The main progress from CMIP5 to CMIP6. *Geosci. Model Dev.* 12, 1573–1600. doi:10.5194/gmd-12-1573-2019.
Wu, X., Che, T., Li, X., Wang, N., and Yang, X. (2018). Slower snowmelt in spring along with climate warming across the Northern Hemisphere. *Geophys. Res. Lett.* doi:10.1029/2018GL079511.
Xia, Y., and Huang, Y. (2017). Differential Radiative Heating Drives Tropical Atmospheric Circulation Weakening. *Geophys. Res. Lett.* 44, 10,592-10,600. doi:10.1002/2017GL075678.
Xiang, T., Vivoni, E. R., and Gochis, D. J. (2018). Influence of initial soil moisture and vegetation conditions on monsoon precipitation events in northwest México. *Atmosfera* 31, 25–45. doi:10.20937/ATM.2018.31.01.03.
Xie, S.-P., Lu, B., and Xiang, B. (2013). Similar spatial patterns of climate responses to aerosol and greenhouse gas changes. *Nat. Geosci.* 6, 828–832. doi:10.1038/ngeo1931.
Yang, Y., Roderick, M. L., Zhang, S., McVicar, T. R., and Donohue, R. J. (2018). Hydrologic implications of vegetation response to elevated CO2 in climate projections. *Nat. Clim. Chang.* 9, 44–48. doi:10.1038/s41558-018-0361-0.
Yin, J., Gentine, P., Zhou, S., Sullivan, S. C., Wang, R., Zhang, Y., et al. (2018). Large increase in global storm runoff extremes driven by climate and anthropogenic changes. *Nat. Commun.* 9, 4389. doi:10.1038/s41467-018-06765-2.
Yukimoto, S., Koshiro, T., Kawai, H., Oshima, N., Yoshida, K., Urakawa, S., et al. (2019). MRI MRI-ESM2.0 model output prepared for CMIP6 CMIP. doi:10.22033/ESGF/CMIP6.621.

Zanardo, S., Nicotina, L., Hilberts, A. G. J., and Jewson, S. P. (2019). Modulation of economic losses from European floods by the North Atlantic Oscillation. *Geophys. Res. Lett.* doi:10.1029/2019GL081956.
Zellou, B., and Rahali, H. (2019). Assessment of the joint impact of extreme rainfall and storm surge on the risk of flooding in a coastal area. *J. Hydrol.* 569, 647–665. doi:10.1016/j.jhydrol.2018.12.028.
Zeng, X., Broxton, P., and Dawson, N. (2018). Snowpack Change From 1982 to 2016 Over Conterminous United States. *Geophys. Res. Lett.* doi:10.1029/2018gl079621.
Zhang, B., and Soden, B. J. (2019). Constraining Climate Model Projections of Regional Precipitation Change. *Geophys. Res. Lett.* 0. doi:10.1029/2019GL083926.
Zhang, X., Zwiers, F. W., Li, G., Wan, H., and Cannon, A. J. (2017). Complexity in estimating past and future extreme short-duration rainfall. *Nat. Geosci.* 10, 255–259. doi:10.1038/ngeo2911.
Zhang, Y., and Fueglistaler, S. (2019). Mechanism for Increasing Tropical Rainfall Unevenness with Global Warming. *Geophys. Res. Lett.* n/a. doi:10.1029/2019GL086058.
Zhang, Z., Ralph, F. M., and Zheng, M. (2018). The Relationship between Extratropical Cyclone Strength and Atmospheric River Intensity and Position. *Geophys. Res. Lett.* 46, 1814–1823. doi:10.1029/2018gl079071.
Zhao, C., Lin, Y., Wu, F., Wang, Y., Li, Z., Rosenfeld, D., et al. (2018a). Enlarging rainfall area of tropical cyclones by atmospheric aerosols. *Geophys. Res. Lett.* doi:10.1029/2018GL079427.
Zhao, M., Golaz, J.-C., Held, I. M., Guo, H., Balaji, V., Benson, R., et al. (2018b). The GFDL Global Atmosphere and Land Model AM4.0/LM4.0: 1. Simulation Characteristics With Prescribed SSTs. *J. Adv. Model. Earth Syst.* 10, 691–734. doi:10.1002/2017MS001208.
Zhou, C., Wang, K., and Qi, D. (2018). 21. Attribution of the July 2016 extreme precipitation event over China's Wuhan. *Bull. Am. Meteorol. Soc.* 99, S107–S112. doi:10.1175/BAMS-D-17-0090.1.
Zhou, W., Xie, S.-P., and Yang, D. (2019a). Enhanced equatorial warming causes deep-tropical contraction and subtropical monsoon shift. *Nat. Clim. Chang.* doi:10.1038/s41558-019-0603-9.
Zhou, Y., Luo, M., and Leung, Y. (2016). On the detection of precipitation dependence on temperature. *Geophys. Res. Lett.* 43, 4555–4565. doi:10.1002/2016GL068811.
Zhou, Y., Sawyer, A. H., David, C. H., and Famiglietti, J. S. (2019b). Fresh submarine groundwater discharge to the near-global coast. *Geophys. Res. Lett.*, 2019GL082749. doi:10.1029/2019GL082749.
Zika, J. D., Skliris, N., Blaker, A. T., Marsh, R., Nurser, A. J. G., and Josey, S. A. (2018). Improved estimates of water cycle change from ocean salinity: The key role of ocean warming. *Environ. Res. Lett.* 13. doi:10.1088/1748-9326/aace42.